Supplementary Information (SI) for New Journal of Chemistry.

Dual Targeted Ugi-Bisamides Induce Caspase Mediated Apoptosis and Inhibit PI3K/mTOR Signaling in NSCLC

Mohammed Salah Ayoup[1,2] *, Khadiga Yousry[2], Hamida Abdel-Hamid[2], Mohamed S. Nafie[3,4], Doaa A. Ghareeb[5,6,7], Aliaa Masoud[5], Marwa F. Harras[8], Jawaher Y. Al Nawah[1], Magda M. F. Ismail[8]* and Gina N. Tageldin[9]*

[1] *Department of Chemistry, College of Science, King Faisal University, Al-Ahsa 31982, Saudi Arabia.*
[2] *Department of Chemistry, Faculty of Science, Alexandria University, Alexandria, Egypt.*
[3] *Department of Chemistry, College of Sciences, University of Sharjah, Sharjah (P.O. 27272), United Arab Emirates (UAE).*
[4] *Chemistry Department, Faculty of Science, Suez Canal University, Ismailia 41522, Egypt.*
[5] *Bio-screening and preclinical trial lab, Biochemistry Department, Faculty of Science, Alexandria University, Alexandria, Egypt.*
[6] *Center of Excellence for Drug Preclinical Studies (CE-DPS), Pharmaceutical and Fermentation Industry Development Center, City of Scientific Research & Technological Applications (SRTA-city), New Borg El Arab, Alexandria, Egypt.*
[7] *Research Projects unit, Pharos University in Alexandria; Canal El Mahmoudia Street, Beside Green Plaza Complex 21648, Alexandria, Egypt.*
[8] *Department of Pharmaceutical Medicinal Chemistry and Drug Design, Faculty of Pharmacy (Girls), Al-Azhar University, Cairo 11754, Egypt.*
[9] *Department of Pharmaceutical Chemistry, Faculty of Pharmacy, Alexandria University, Alexandria, 21521, Egypt.*
**Corresponding author*
Email addresses: mayoup@kfu.edu.sa , m.elalfy101@gmail.com, gina.tageldin@alexu.edu.eg..

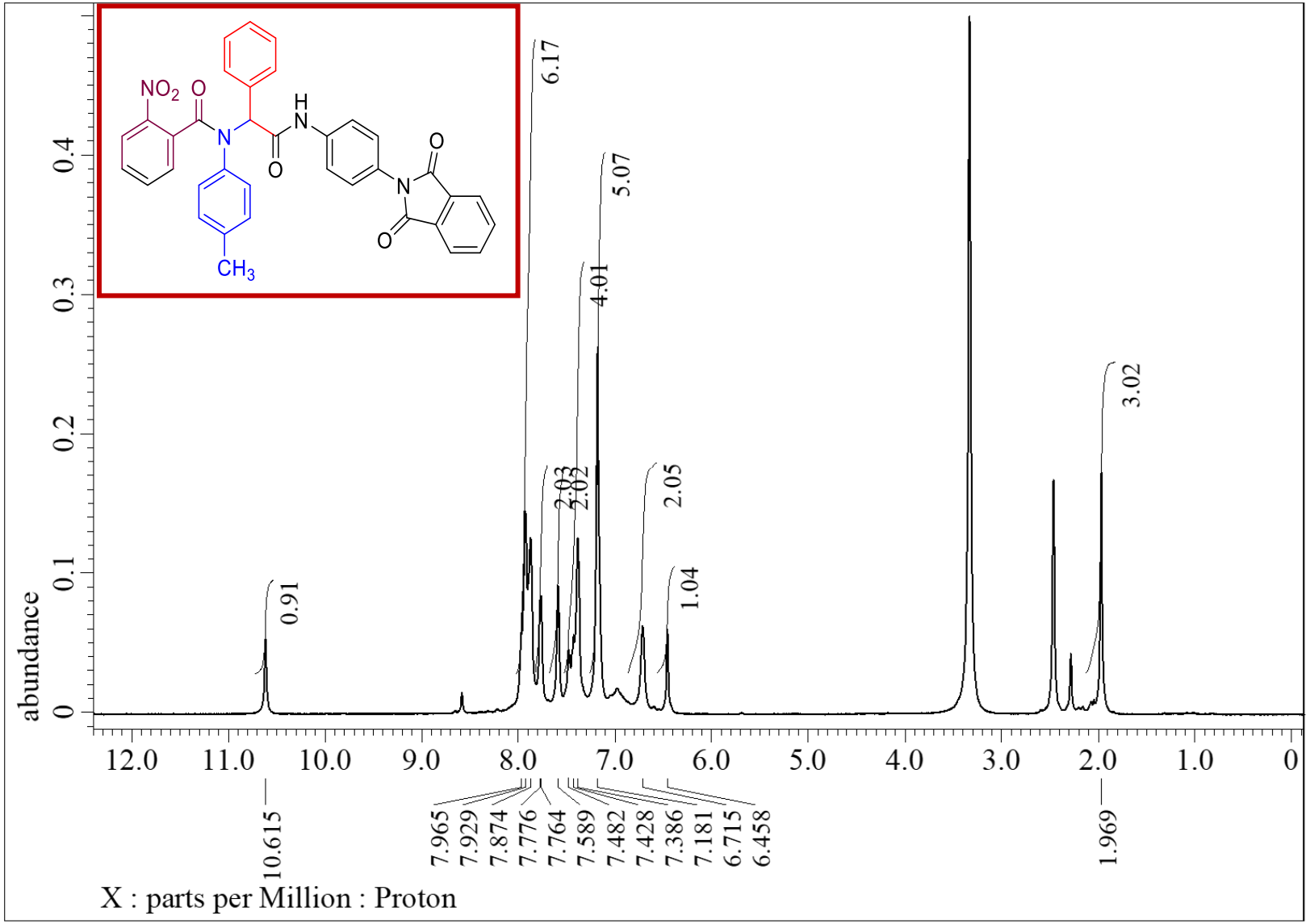

Figure S1. ^{1}H-NMR (500 MHz, DMSO-d_6) spectrum of **5**

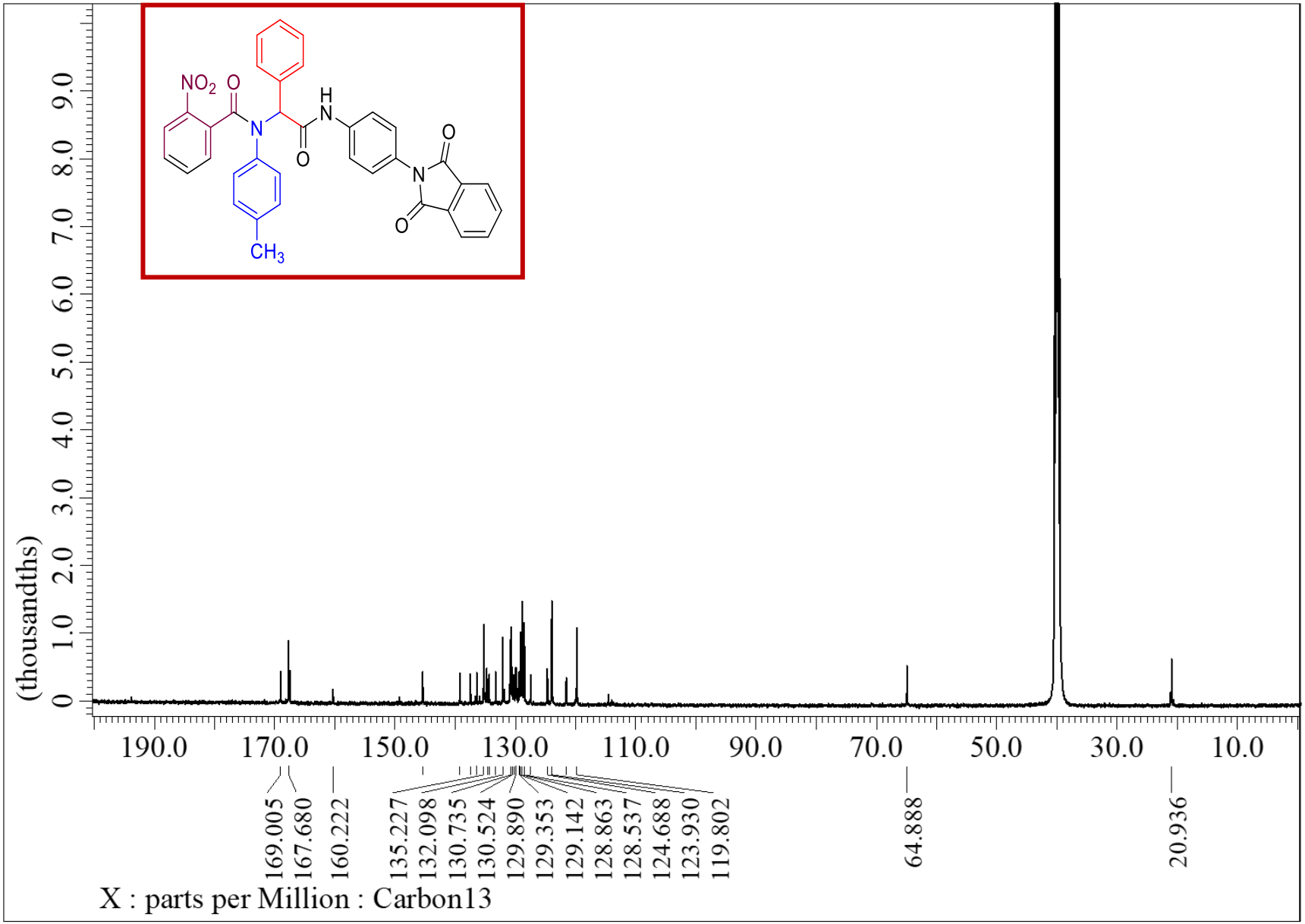

Figure S2. ^{13}C-NMR (125 MHz, DMSO-d_6) spectrum of **5**

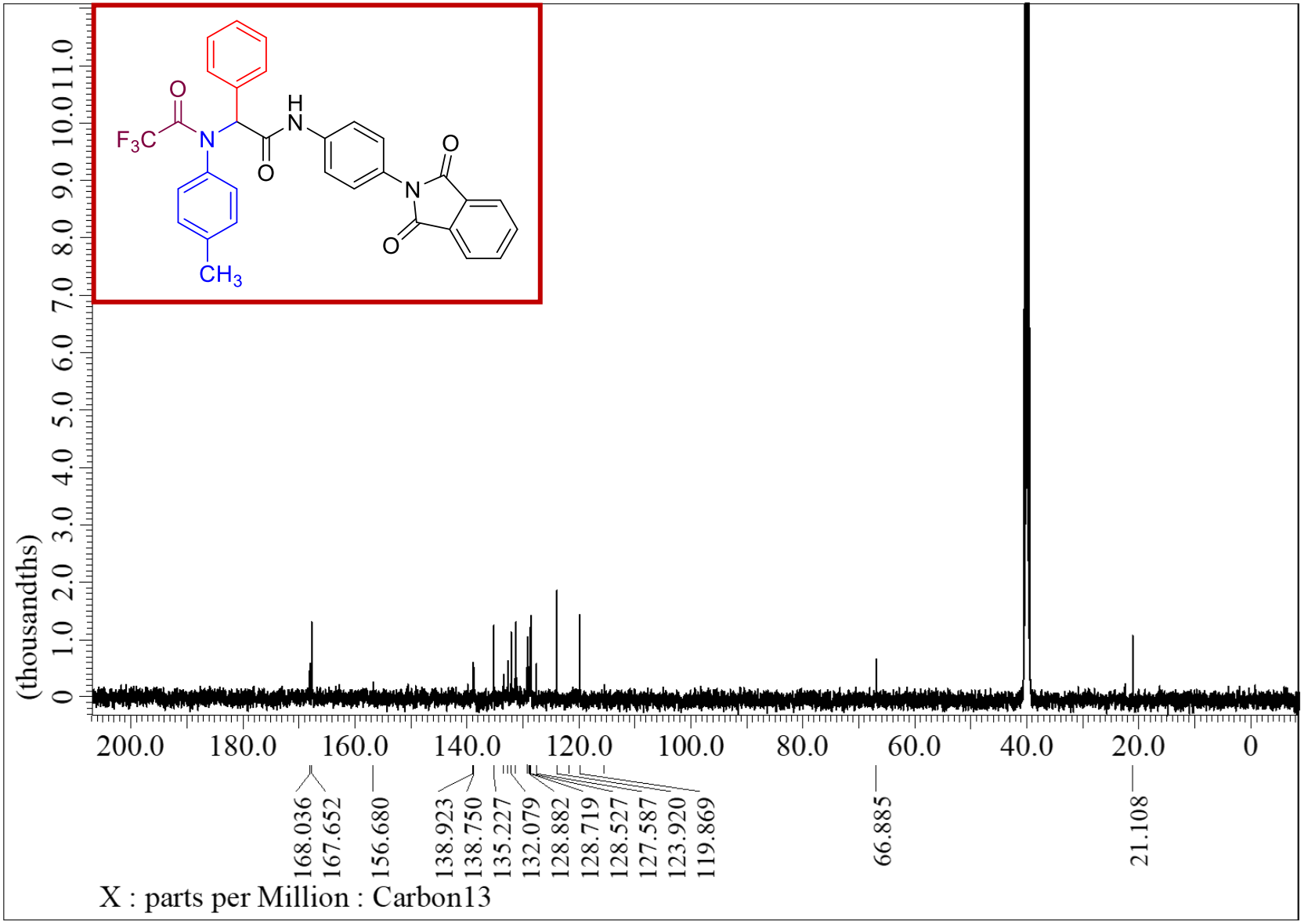

Figure S3. ^{13}C-NMR (125 MHz, DMSO-d_6) spectrum of **6**

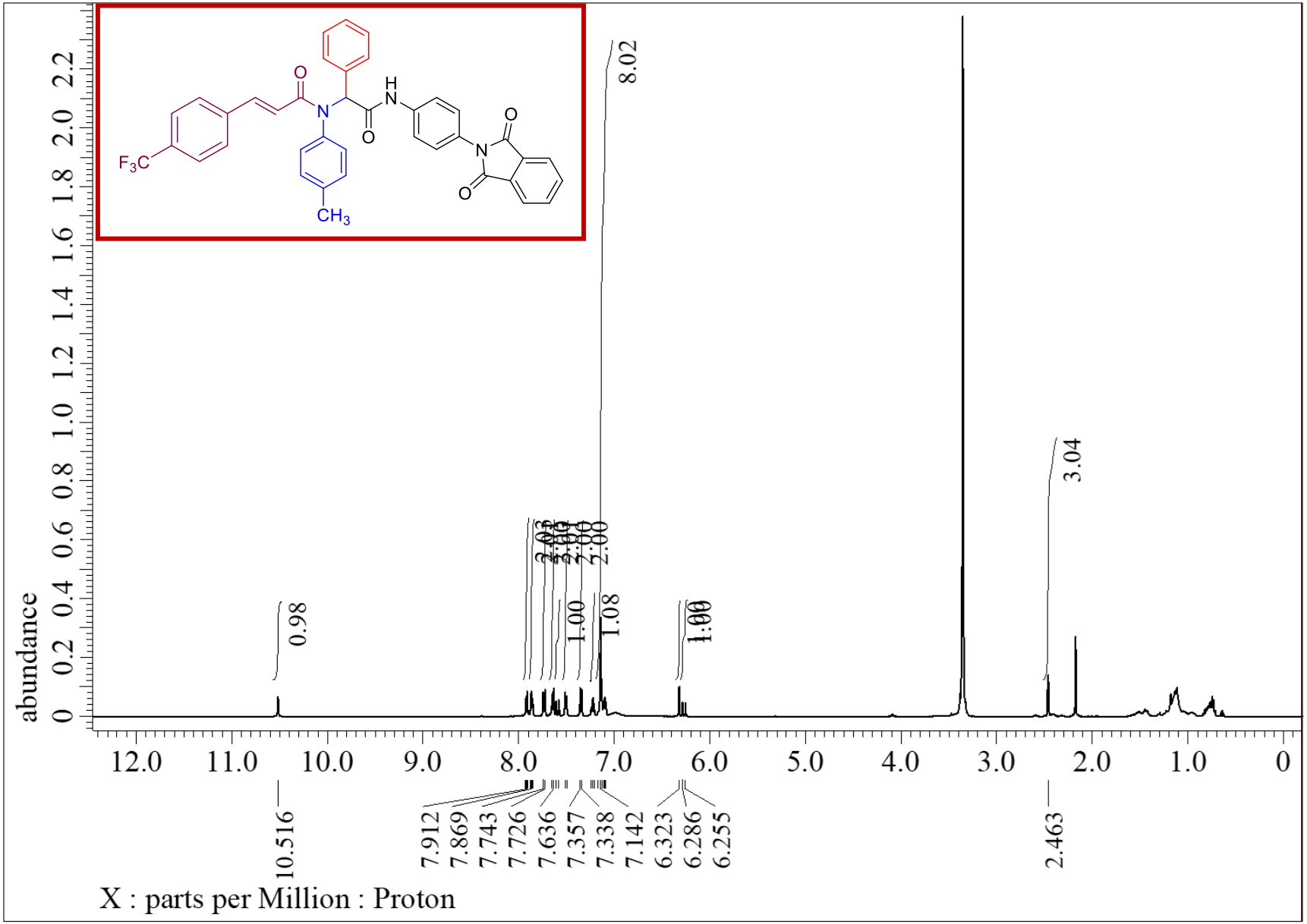

Figure S4. ^{1}H-NMR (500 MHz, DMSO-d_6) spectrum of **7**

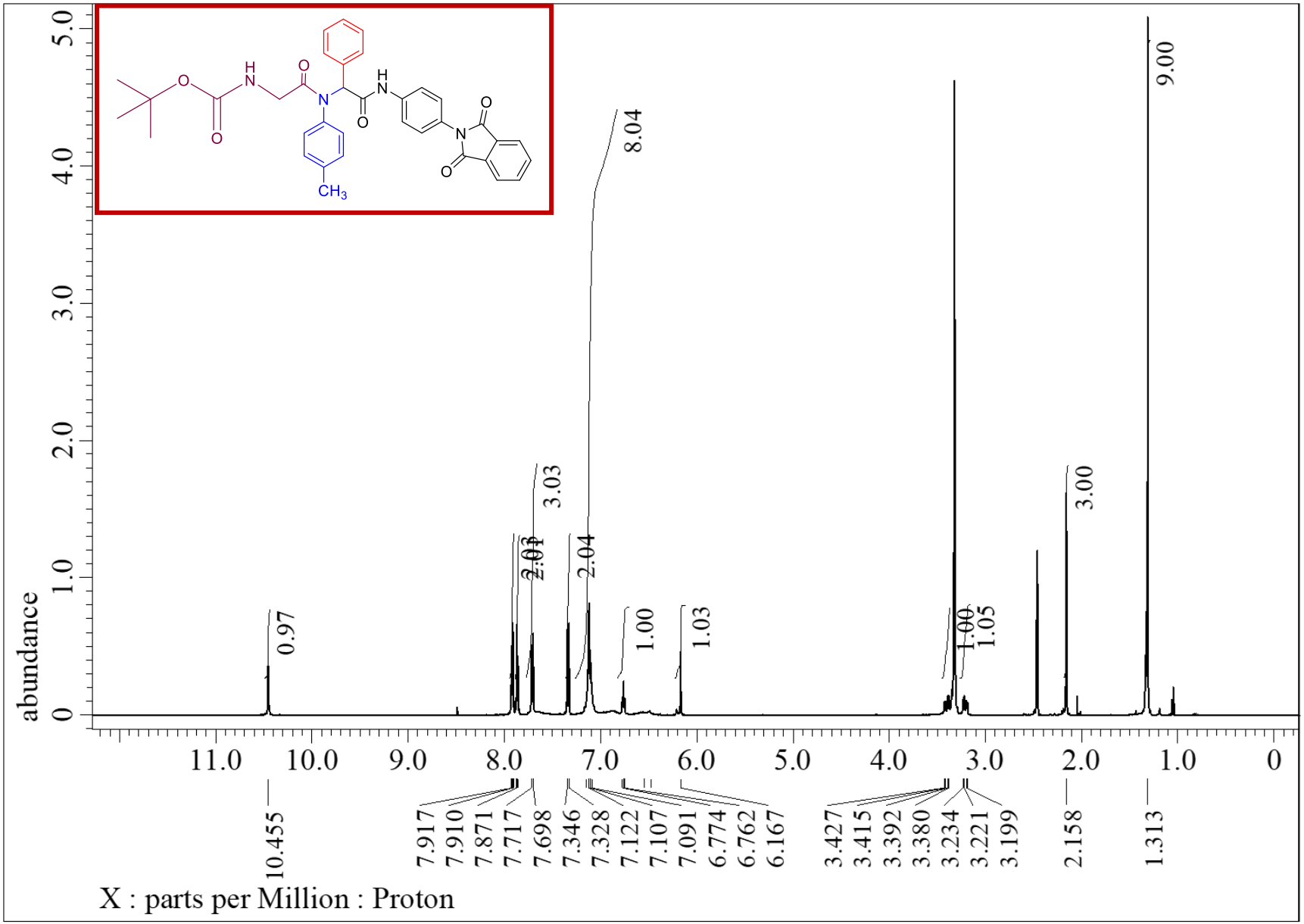

Figure S5. ^{1}H-NMR (500 MHz, DMSO-d_6) spectrum of **8**

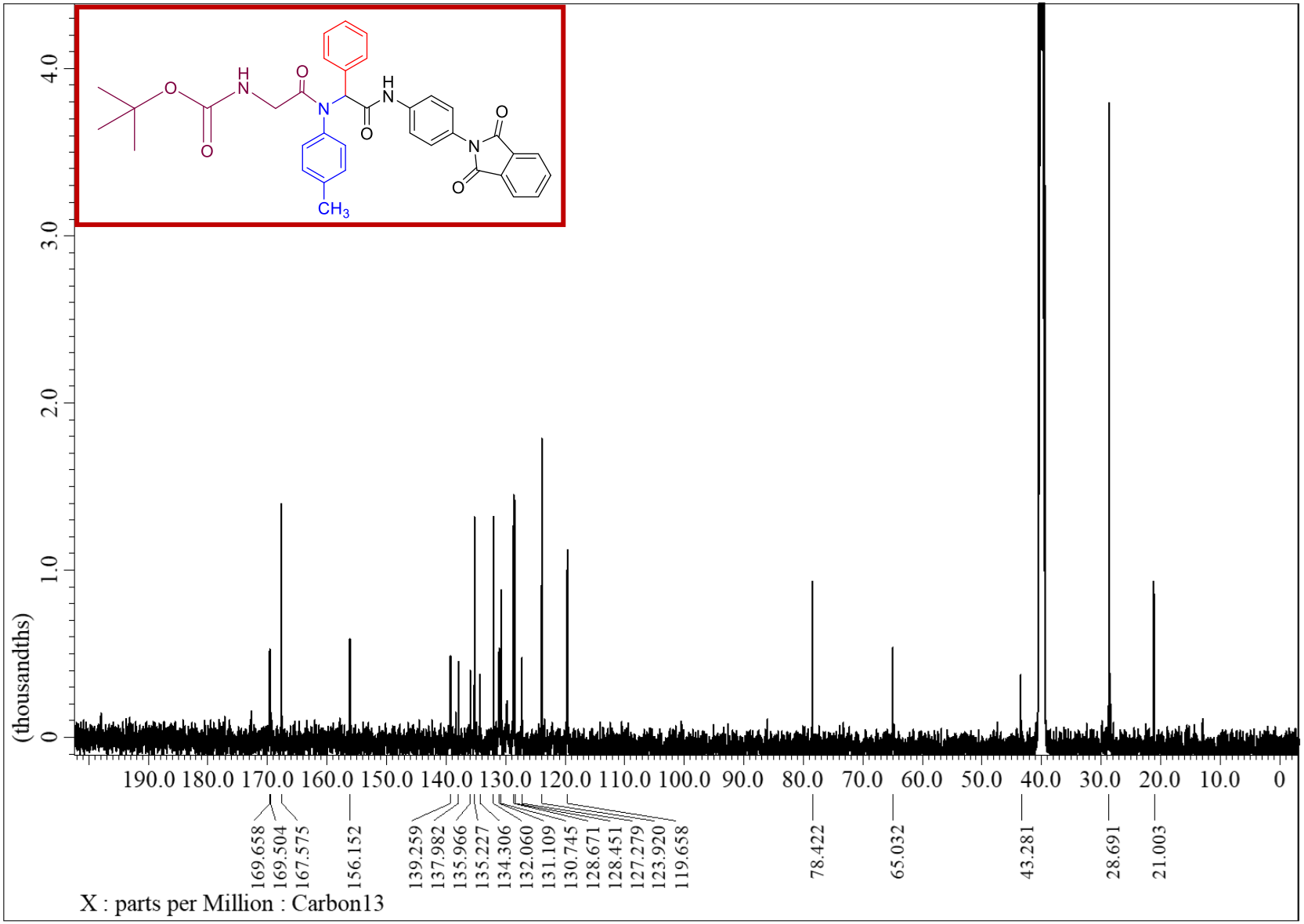

Figure S6. ^{13}C-NMR (125 MHz, DMSO-d_6) spectrum of **8**

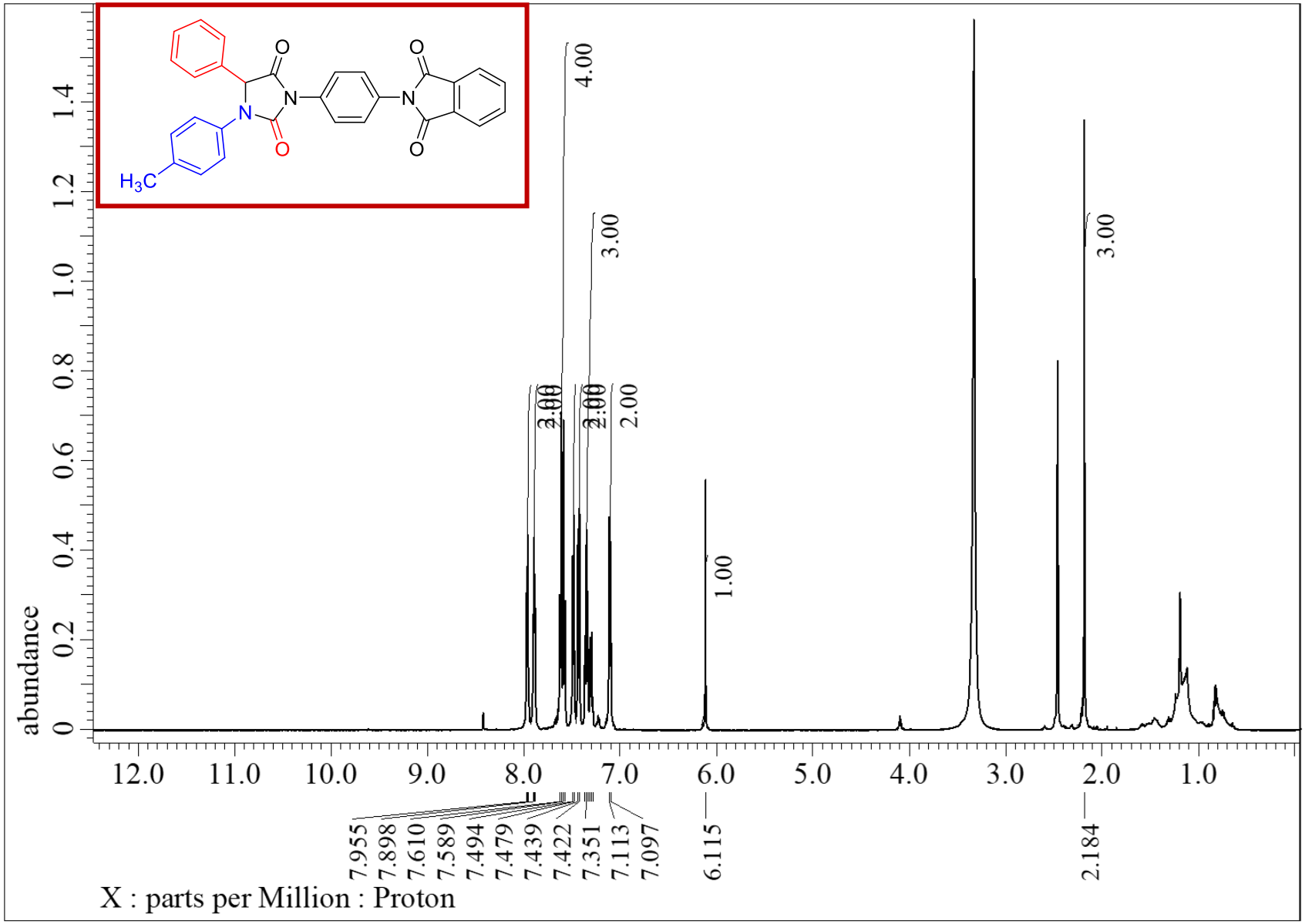

Figure S7. ^{1}H-NMR (500 MHz, DMSO-d_6) spectrum of **11**

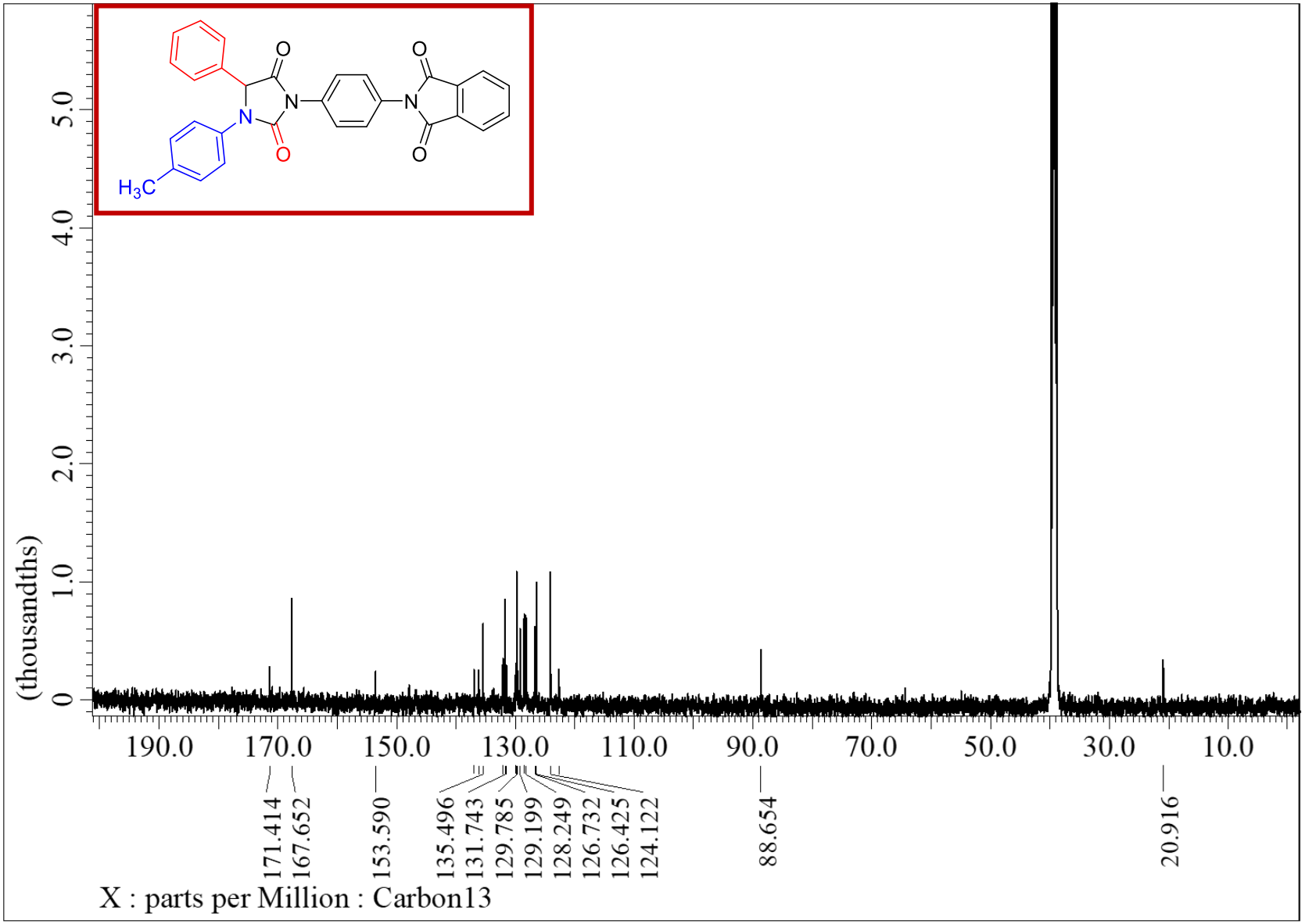

Figure S8. ^{13}C-NMR (125 MHz, DMSO-d_6) spectrum of **11**

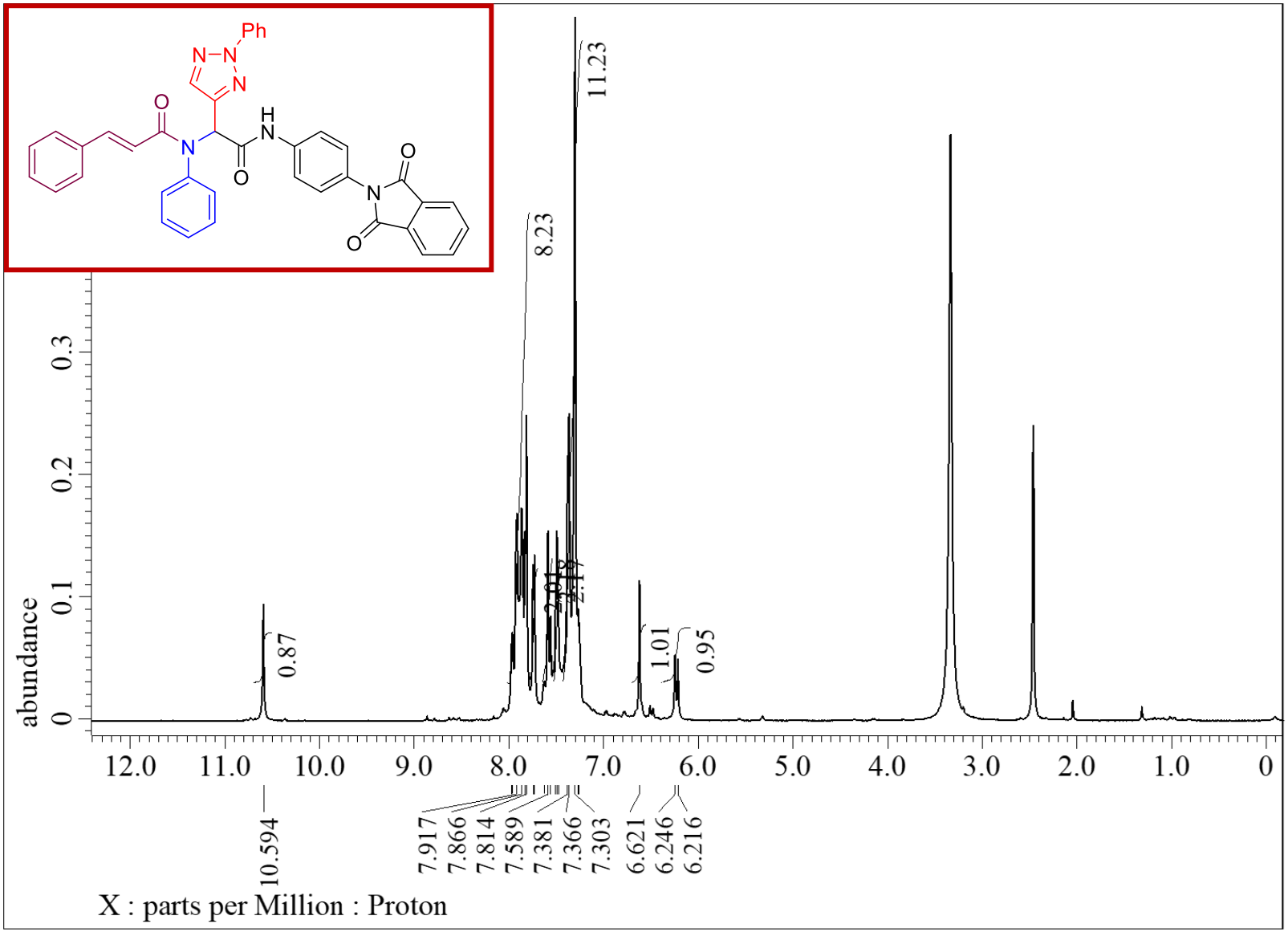

Figure S9. ^{1}H-NMR (500 MHz, DMSO-d_6) spectrum of **12**

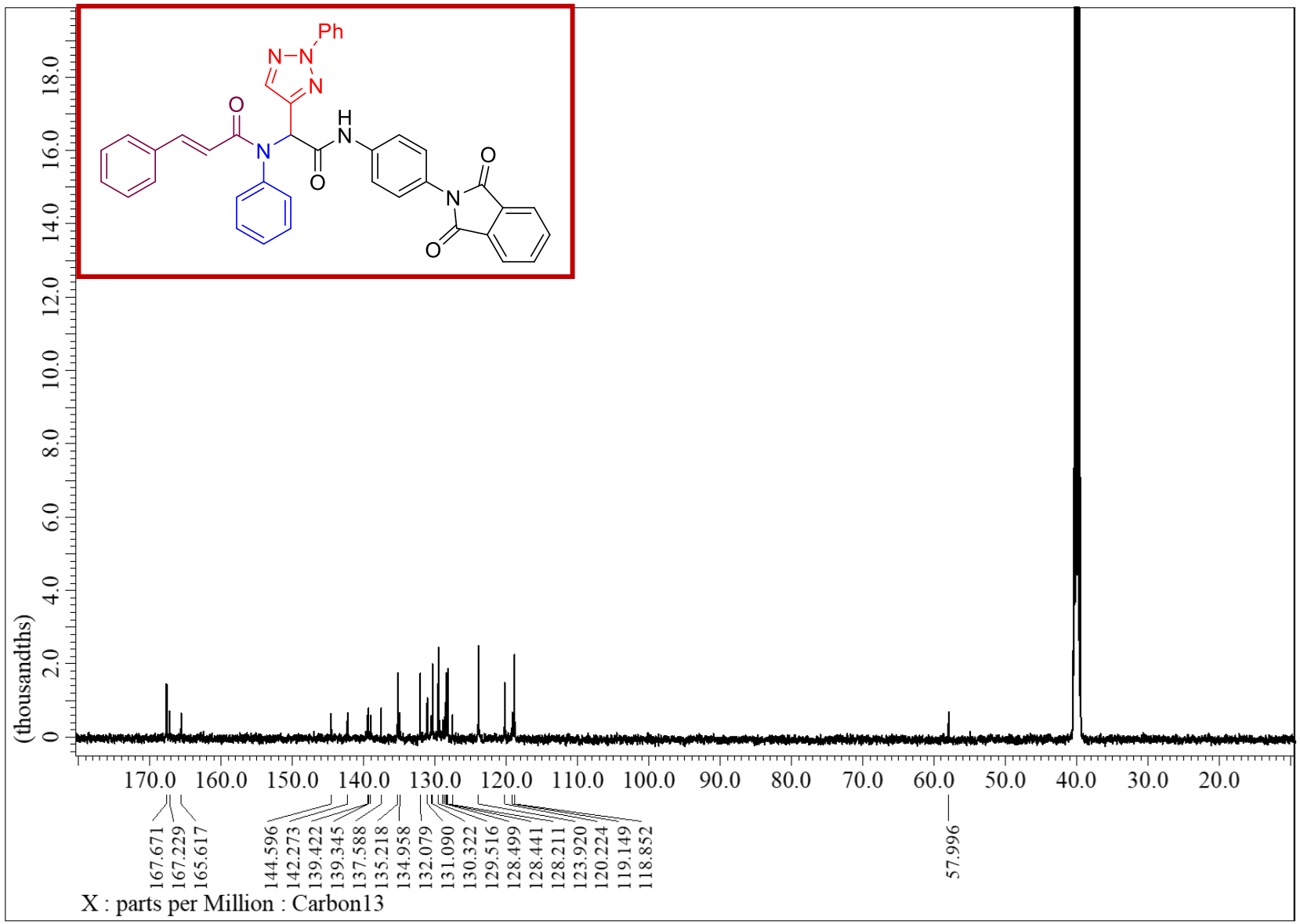

Figure S10. ^{13}C-NMR (125 MHz, DMSO-d_6) spectrum of **12**

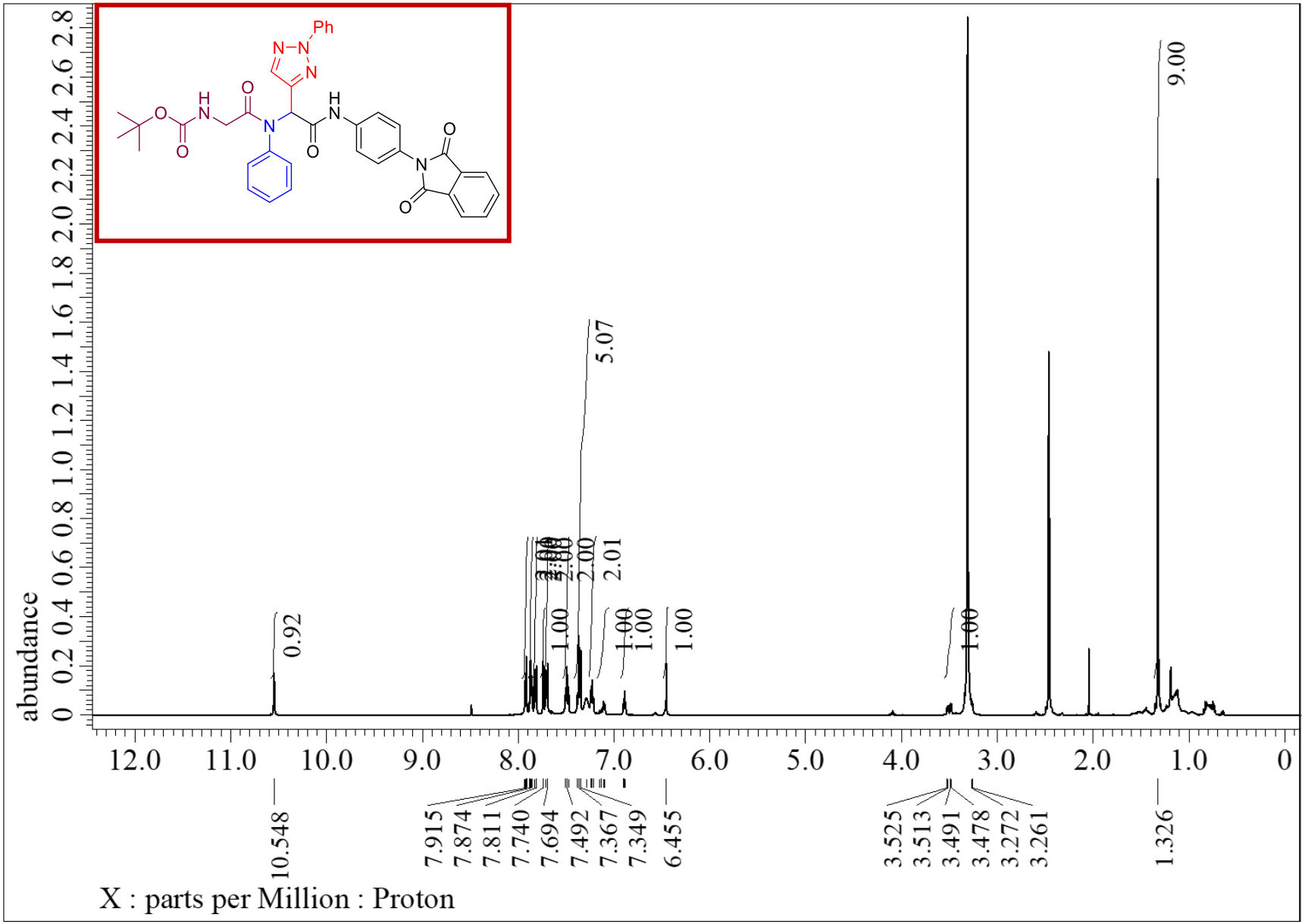

Figure S11. ^{1}H-NMR (500 MHz, DMSO-d_6) spectrum of **13**

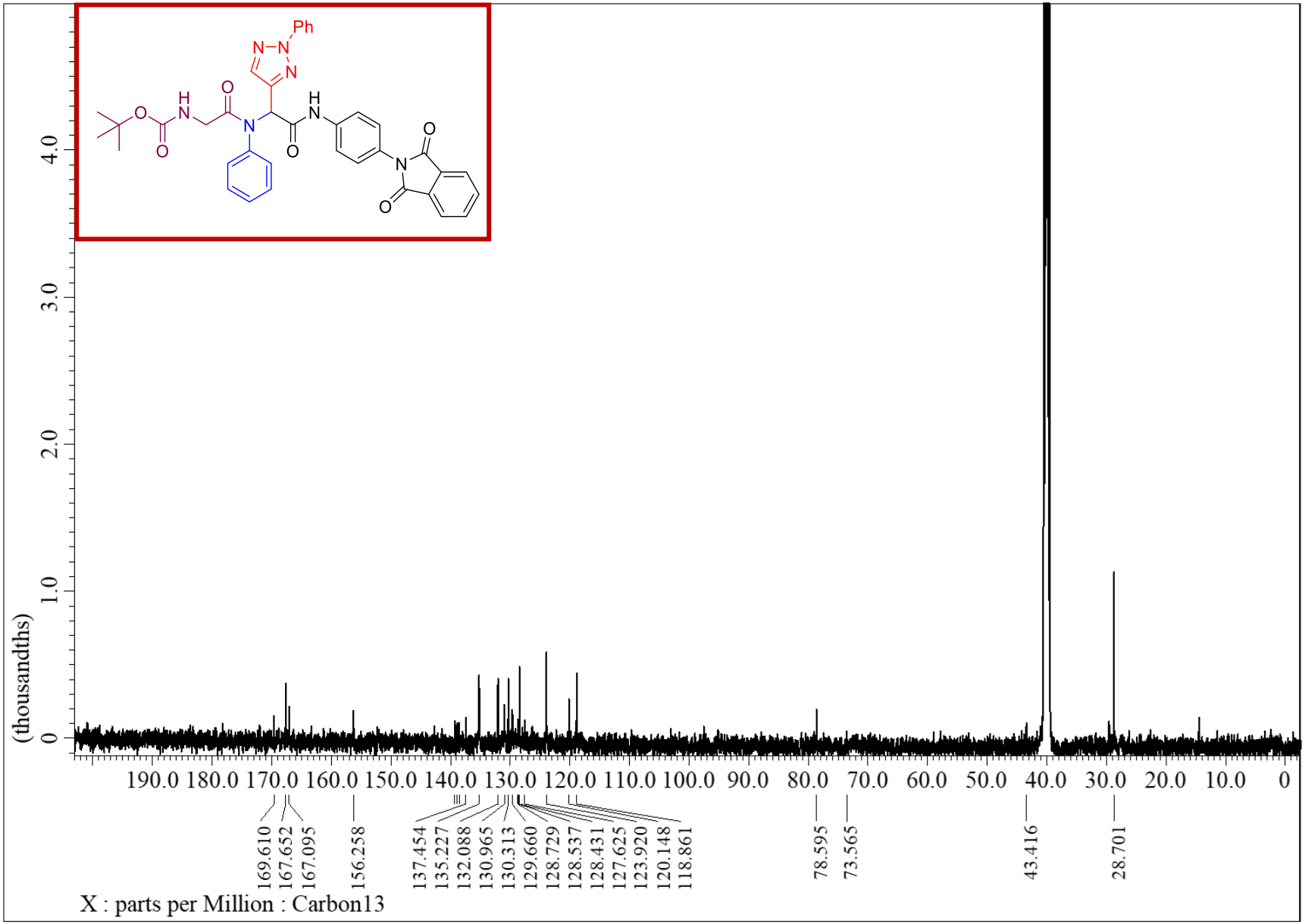

Figure S12. ^{13}C-NMR (125 MHz, DMSO-d_6) spectrum of **13**

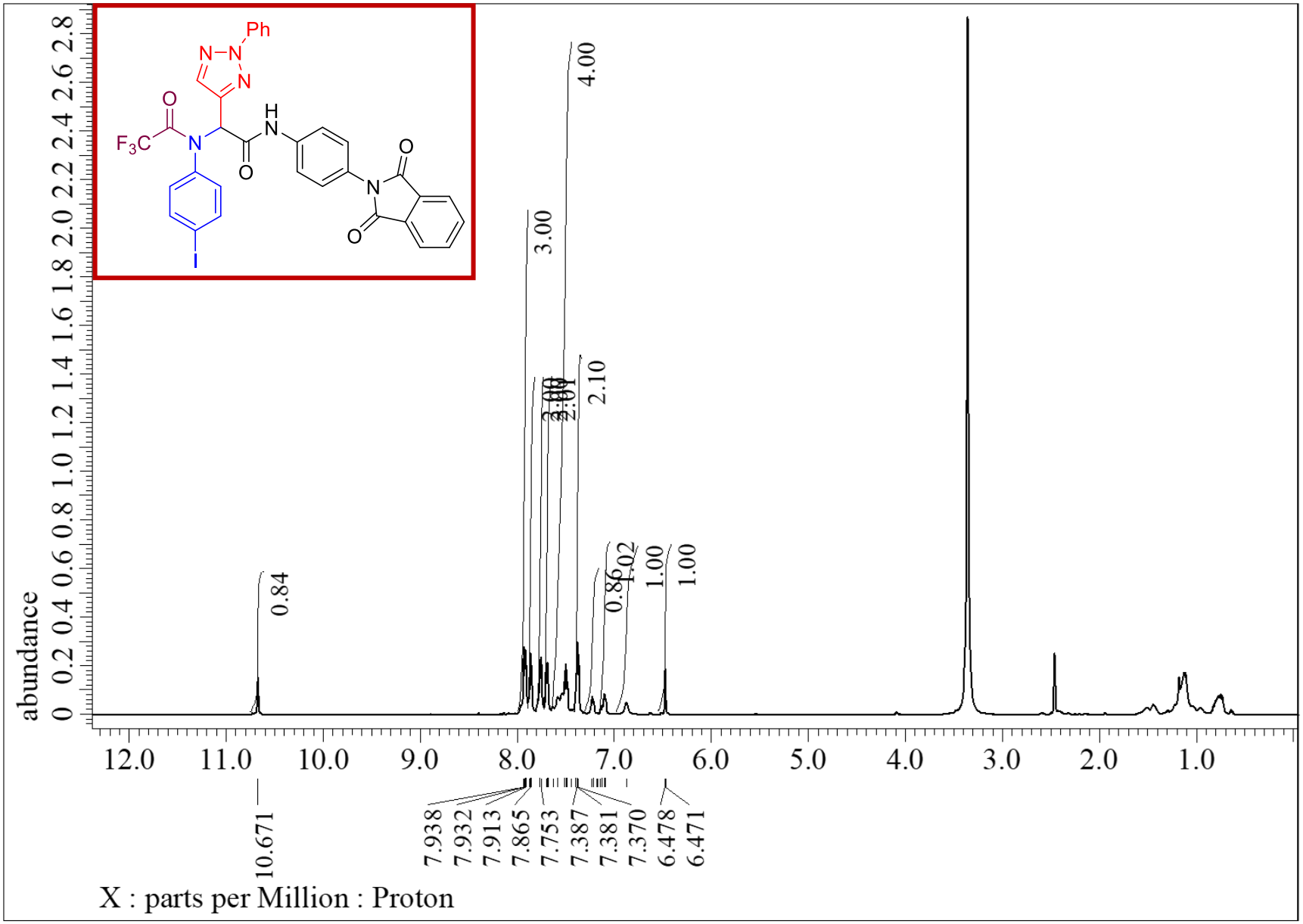

Figure S13. ^{1}H-NMR (500 MHz, DMSO-d_6) spectrum of **16**

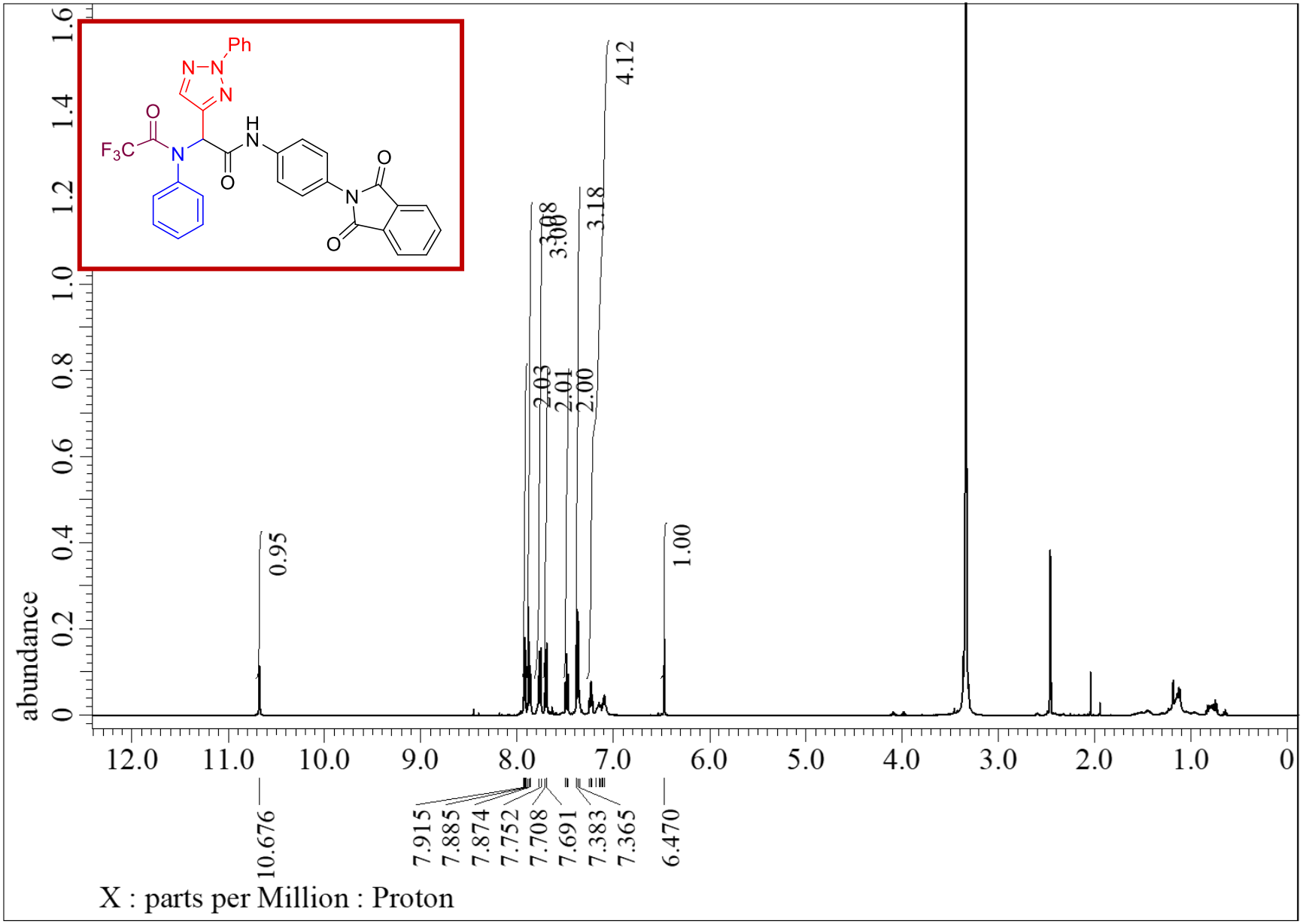

Figure S14. ^{1}H-NMR (500 MHz, DMSO-d_6) spectrum of **17**

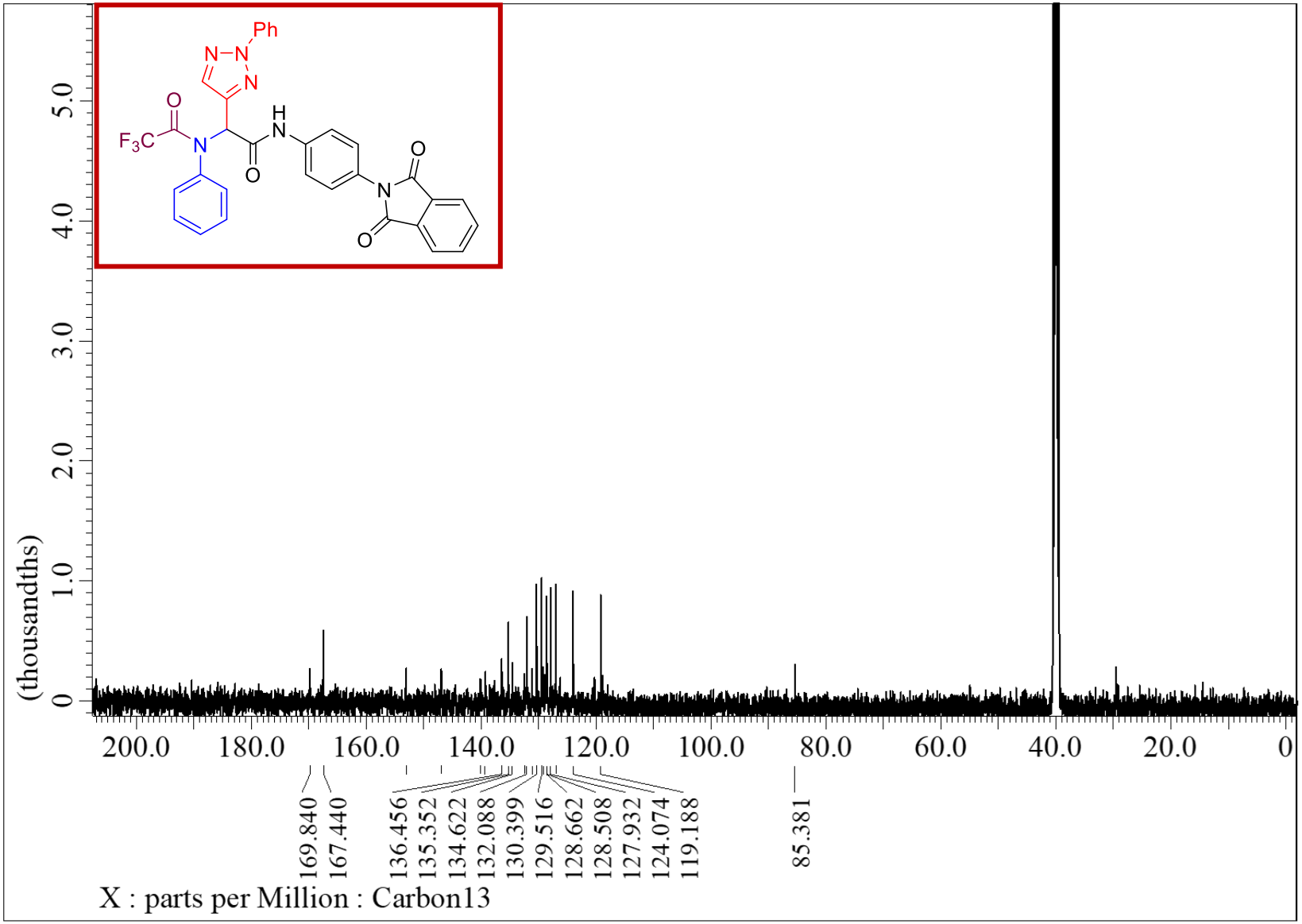

Figure S15. ^{13}C-NMR (125 MHz, DMSO-d_6) spectrum of **17**

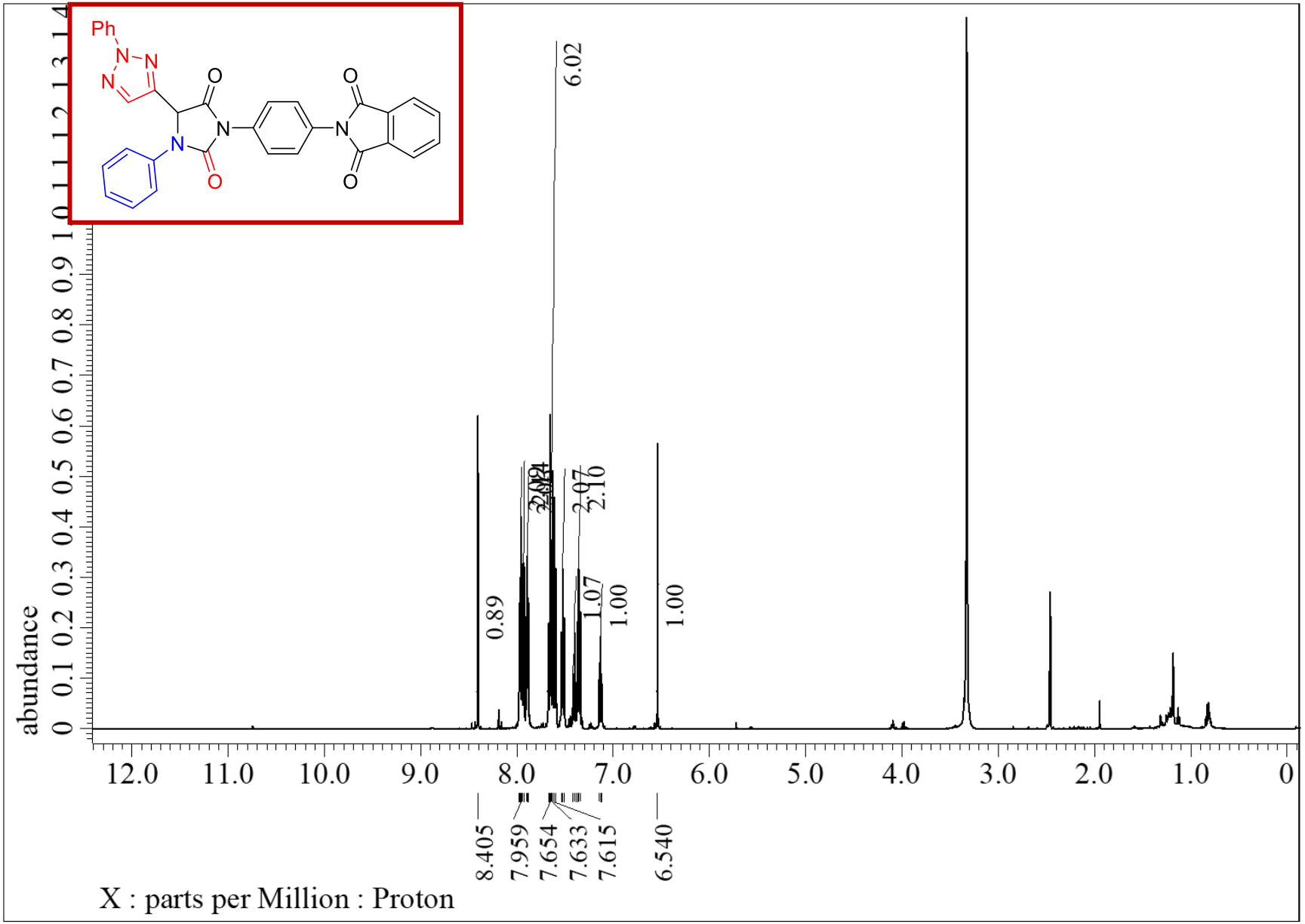

Figure S16. ^{1}H-NMR (500 MHz, DMSO-d_6) spectrum of **18**

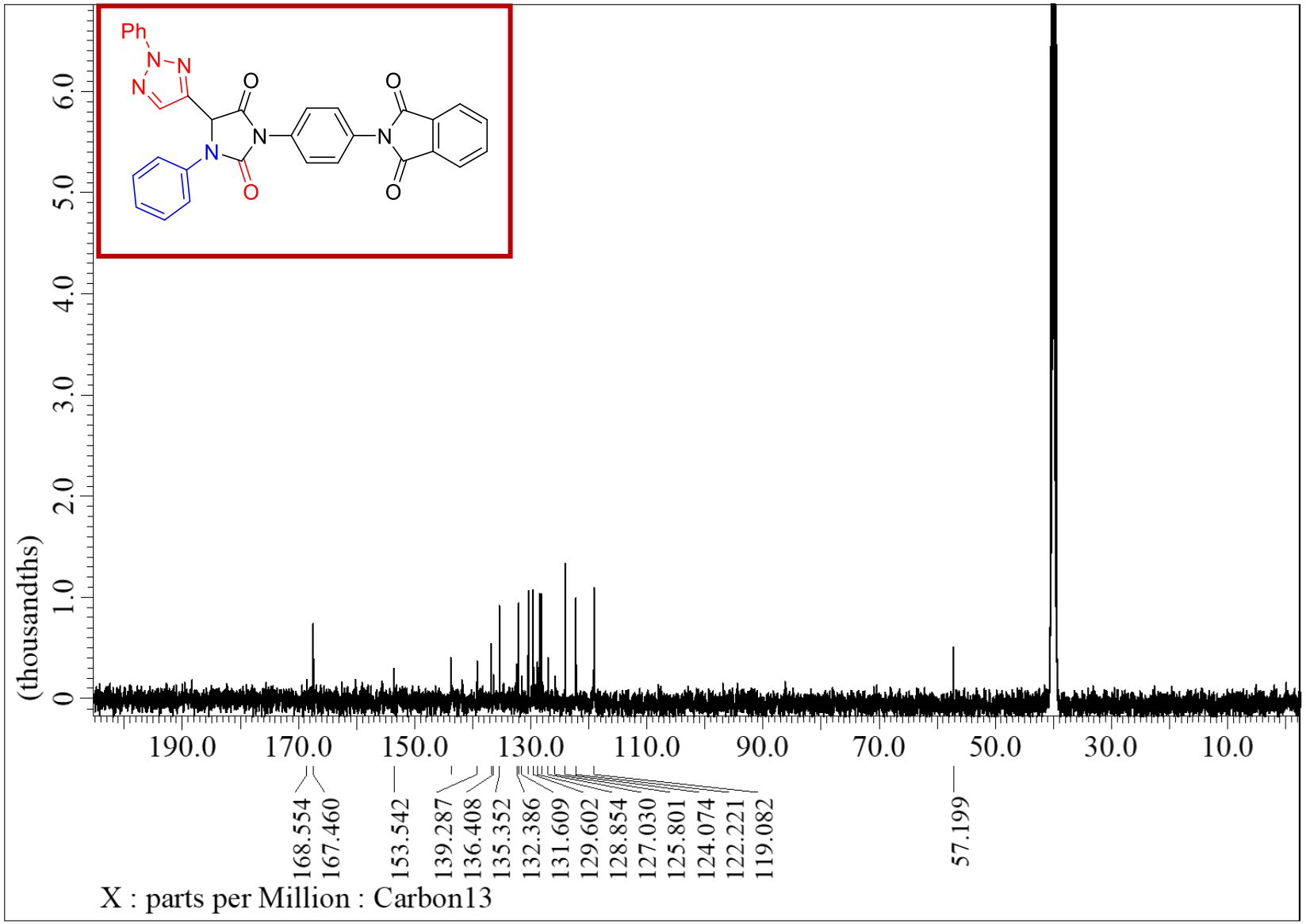

Figure S17. ^{13}C-NMR (125 MHz, DMSO-d_6) spectrum of **18**

2. Material and Equipment

All starting compounds were commercially purchased. Reactions were performed in dried glassware. NMR spectra were recorded on a 500 MHz JEOLJNM ECA spectrometer. ^{13}C NMR spectra were obtained at 125 MHz. Chemical shifts (δ) were reported in ppm. Melting points were recorded using Thermo Scientific1002D apparatus (220-240V, 200W, 50/60 Hz) and were uncorrected. IR spectra [ν_{max} /cm^{-1}] were recorded using PerkinElmer; FT-IR Spectrum BX and Bruker tensor 37 FT-IR.

3. Biological evaluation

3.1. Cytotoxic evaluation (IC_{50}) on normal lung fibroblast WI-38 and A549 cell lines:

The anticancer evaluation was performed via MTT assay.[1] Briefly, a 200 µL suspension of A549 (ATCC: CCL-185) or WI-38 (ATCC: CCL-25) cells containing 3000 cells/well was plated in a 96-well plate and incubated for 24 h. After incubation, 100 µL of different concentrations of the test compounds in RPMI medium without fetal bovine serum (FBS) was added, and the plate was re-incubated for an additional 24 h in a CO_2 incubator (37°C, 5% CO_2, and 90% relative humidity). After the 24 h incubation, 20 µL of MTT solution (5 mg/ml in PBS) was added to each well, and the plates were incubated for an additional 3 h in the CO_2 incubator to allow the MTT to react.

After the incubation, the plates were centrifuged at 1650 rpm for 10 min, and the medium was discarded. The formazan crystals (MTT by-product) were re-suspended in 100 µL of Dimethylsulfoxide (DMSO, 0.1%), and the absorbance was measured at a wavelength of 570 nm using an Optima spectrophotometer to detect the safe dose that results in 100% cell viability.

The cytotoxicity of the compounds was expressed as IC_{50} and calculated using Quest Graph™ IC_{50} Calculator,[2] based on the % inhibition calculated from the serial dilutions of each test compound.

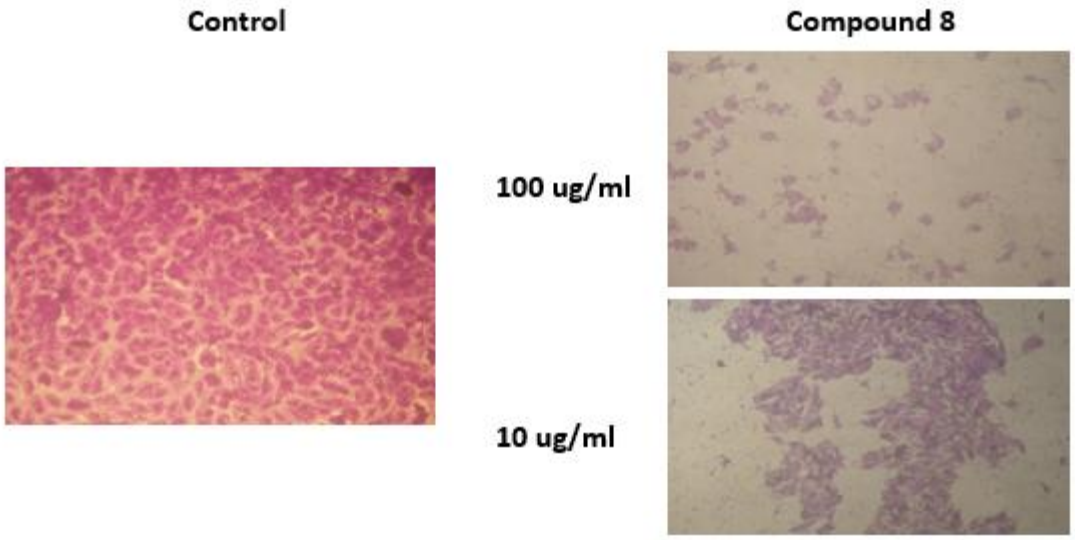

Figure S18. Morphological changes in the untreated and treated A549 cancer cells for the most cytotoxic compound.

Table S1. % inhibition of WI-38 cells treated by serial concentrations of the test compounds to calculate their IC_{50} values

Treatment With WI-38 lung normal cells

5			6			7			8		
concentration (ug/ml)	inhibition %	SD	concentration (ug/ml)	inhibition %	SD	concentration (ug/ml)	inhibition %	SD	concentration (ug/ml)	inhibition %	SD
100	64	**6.4**	100	66	5.1	100	79	10.1	100	80	10.9
50	64	3.8	50	60	8.4	50	69	9.8	50	70	9.4
25	56	1.9	25	45	5.7	25	53	8.1	25	61	6.7
12.5	38	2.4	12.5	40	2.9	12.5	41	6.6	12.5	50	8.1
6.24	23	5.4	6.24	23	1.8	6.24	34	5.6	6.24	33	4.7
3.12	11	0.8	3.12	18	1.9	3.12	9	0.8	3.12	11	0.8
IC50	18.96	2.8	IC50	28.11	3.2	IC50	18.05	2.3	IC50	13.1	1.9

9			10			11			12		
concentration (ug/ml)	inhibition %	SD	concentration (ug/ml)	inhibition %	SD	concentration (ug/ml)	inhibition %	SD	concentration (ug/ml)	inhibition %	SD
100	73	**6.8**	100	81	8.8	100	78	6.8	100	82	**9.4**
50	73	4.5	50	71	6.9	50	67	8.3	50	82	6.5
25	65	7.8	25	58	4.6	25	58	7.9	25	74	9.4
12.5	47	5.6	12.5	35	1.6	12.5	45	3.9	12.5	56	6.4
6.24	32	0.9	6.24	21	2.4	6.24	31	2.8	6.24	41	3.4
3.12	5	0.4	3.12	15	0.9	3.12	18	1.2	3.12	14	0.8
IC50	12.35	2.8	IC50	20.12	2.9	IC50	16.6	2.8	IC50	8.82	1.3

13			14			15			16		
concentration (ug/ml)	inhibition %	SD	concentration (ug/ml)	inhibition %	SD	concentration (ug/ml)	inhibition %	SD	concentration (ug/ml)	inhibition %	SD
100	77	**9.7**	100	70	10	100	90	9.7	100	76	5.9
50	77	8.5	50	70	8.2	50	81	10.8	50	58	7.4
25	69	7.3	25	69	6.8	25	69	6.8	25	46	6.5
12.5	51	6	12.5	56	6.2	12.5	53	3.5	12.5	32	2.9
6.24	36	4.7	6.24	49	4.7	6.24	41	4.8	6.24	19	1.5
3.12	9	0.7	3.12	30	1.7	3.12	29	1.9	3.12	11	1.1
IC50	10.55	0.87	IC50	7.04	0.64	IC50	10.23	0.97	IC50	32.05	4.6

17			18			sorafenib		
concentration (ug/ml)	inhibition %	SD	concentration (ug/ml)	inhibition %	SD	concentration (ug/ml)	inhibition %	SD
100	80	9.8	100	83	2.6	100	100	12.4
50	73	7.2	50	75	10.1	50	80	9.5
25	66	3.8	25	70	8.1	25	43	5.7
12.5	51	4.2	12.5	61	6.1	12.5	26	3.2
6.24	36	4.8	6.24	49	2.8	6.25	25	2.6
3.12	23	1.5	3.12	37	4.1	3.12	20	1.9
IC50	11.73	1.2	IC50	6.45	0.97	IC50	89.52	9.3

Table S2. % inhibition of A549 cancer cells treated by serial concentrations of the test compounds to calculate their IC_{50} values

Treatment With A549 lung cancer cells

5			6			7			8		
concentration (ug/ml)	inhibition %	**SD**	concentration (ug/ml)	inhibition %	**SD**	concentration (ug/ml)	inhibition %	**SD**	concentration (ug/ml)	inhibition %	**SD**
20	88	**6.4**	20	85	4.3	20	100	7.2	20	98	11.7
10	76	3.8	10	83	5.9	10	81	10.4	10	91	10.6
5	64	1.9	5	63	8.1	5	66	7.5	5	83	9.7
2.5	51	2.4	2.5	51	6.5	2.5	59	3.5	2.5	73	6.5
1.25	33	5.4	1.25	33	2.3	1.25	43	4.1	1.25	65	7.2
0.625	25	0.8	0.625	8	1.4	0.625	16	2.3	0.625	38	4.1
IC50	2.61	0.34	IC50	2.39	0.34	IC50	1.99	1.1	IC50	0.86	0.06

9			10			11			12		
concentration (ug/ml)	inhibition %	**SD**	concentration (ug/ml)	inhibition %	**SD**	concentration (ug/ml)	inhibition %	**SD**	concentration (ug/ml)	inhibition %	**SD**
20	85	**6.8**	20	100	9.8	20	87	7.4	20	93	**9.4**
10	73	4.5	10	83	7.6	10	77	6.3	10	82	6.5
5	69	7.8	5	69	6.4	5	63	6.9	5	74	9.4
2.5	50	5.6	2.5	51	6.1	2.5	41	6.3	2.5	66	6.4
1.25	44	0.9	1.25	30	4.2	1.25	18	4.8	1.25	35	3.4
0.625	23	0.4	0.625	18	2.3	0.625	0.5	0.06	0.625	22	0.8
IC50	2.03	0.19	IC50	2.54	0.18	IC50	3.28	0.45	IC50	1.78	0.21

13			14			15			16		
concentration (ug/ml)	inhibition %	SD	concentration (ug/ml)	inhibition %	SD	concentration (ug/ml)	inhibition %	SD	concentration (ug/ml)	inhibition %	SD
20	89	8.4	20	87	7.6	20	93	8.6	20	42	6.4
10	71	6.3	10	65	6.2	10	82	7.2	10	28	3.2
5	59	5.7	5	43	5.7	5	62	5.9	5	17	2.1
2.5	38	4.2	2.5	21	3.4	2.5	43	5.1	2.5	12.5	1.9
1.25	22	3.1	1.25	13	2.2	1.25	31	4.3	1.25	6	0.9
0.625	10	1.3	0.625	6	0.96	0.625	17	2.2	0.625	0	0
IC50	3.9	0.49	IC50	7.9	1.2	IC50	3.11	0.26	IC50	29.5	1.9

17			18			sorafenib		
concentration (ug/ml)	inhibition %	SD	concentration (ug/ml)	inhibition %	SD	concentration (ug/ml)	inhibition %	SD
20	83	6.9	20	78	6.3	20	83.7	9.7
10	69	4.7	10	63	5.7	10	79.9	6.8
5	49	5.3	5	54	3.9	5	66.8	7.6
2.5	34	2.4	2.5	37	4.2	2.5	52.2	6.5
1.25	23	2.6	1.25	20	2.6	1.25	38.4	4.8
0.625	16	1.3	0.625	4	0.3	0.625	25.6	3.9
IC50	5.001	0.23	IC50	4.52	0.38	IC50	2.22	0.31

Table S3. Dose-repose curves for WI-38 and A549 cells treated by serial concentrations of the test compounds to calculate their IC_{50} values

Cpd No.	IC_{50} WI-38	IC_{50} A549
5	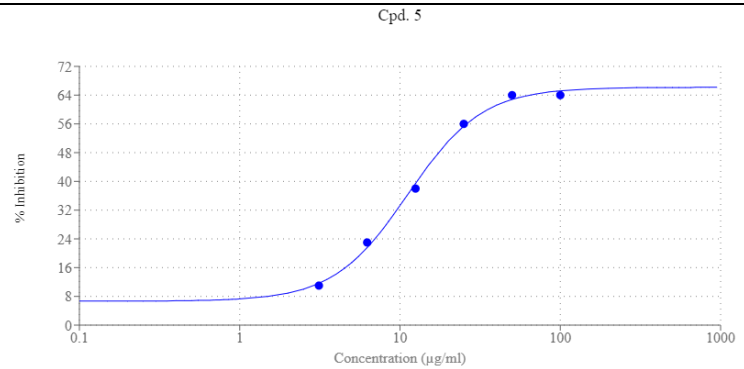	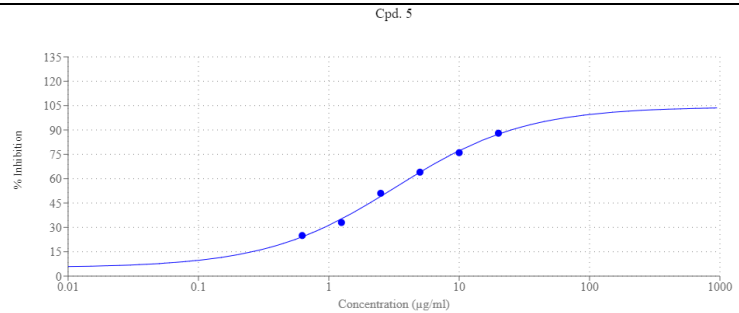
6	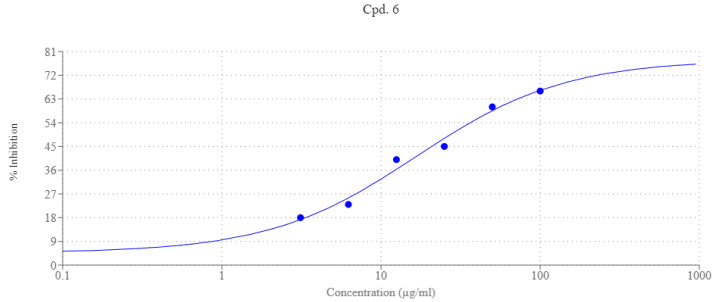	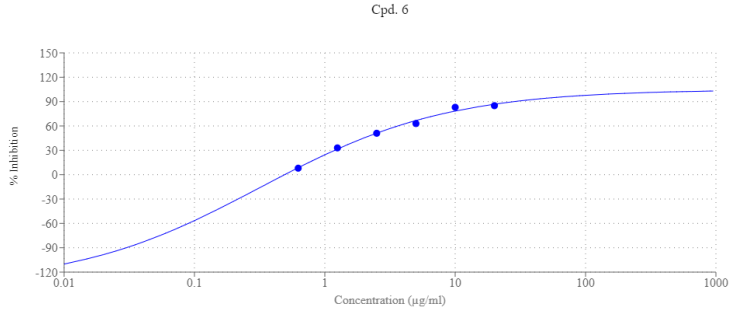
7	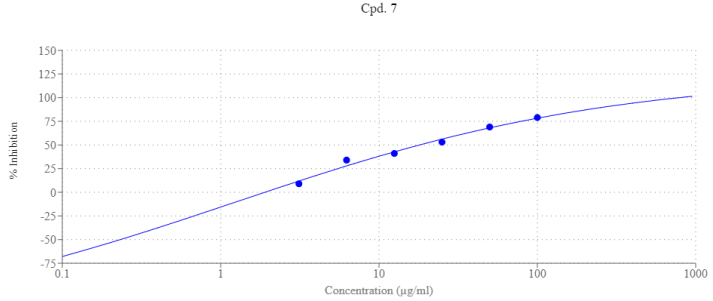	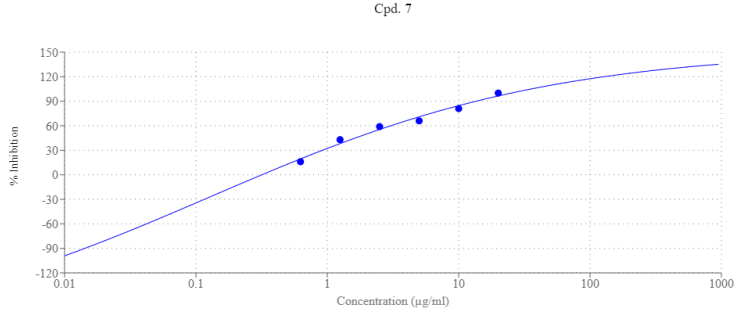

8	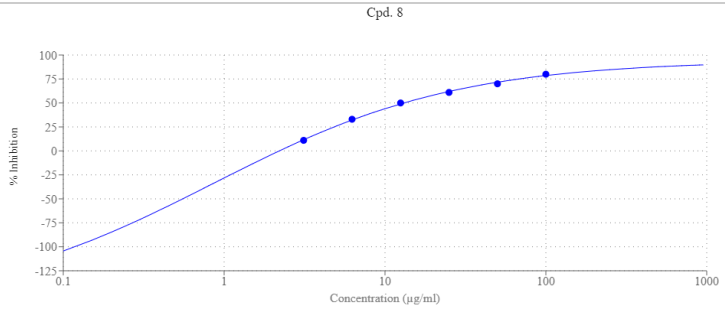 Cpd. 8 % Inhibition Concentration (µg/ml)	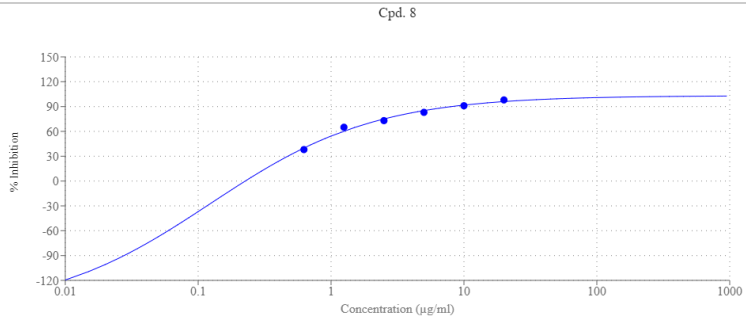 Cpd. 8 % Inhibition Concentration (µg/ml)
9	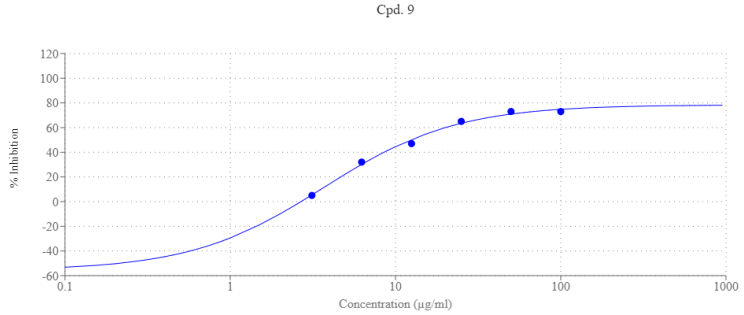 Cpd. 9 % Inhibition Concentration (µg/ml)	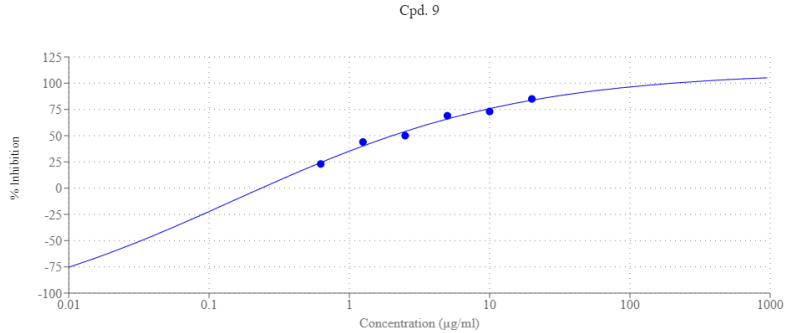 Cpd. 9 % Inhibition Concentration (µg/ml)
10	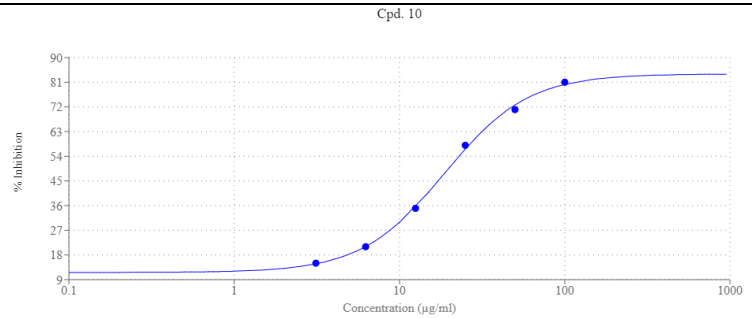 Cpd. 10 % Inhibition Concentration (µg/ml)	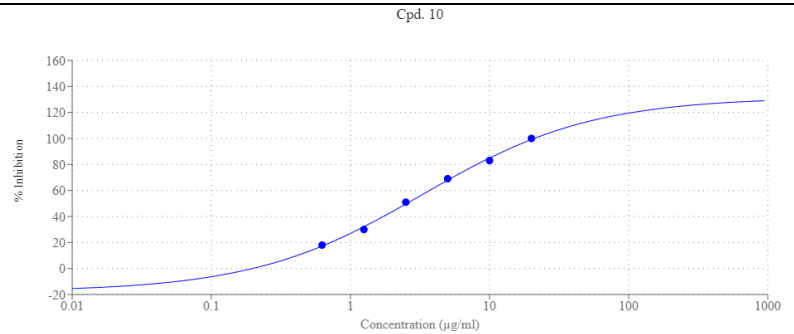 Cpd. 10 % Inhibition Concentration (µg/ml)
11	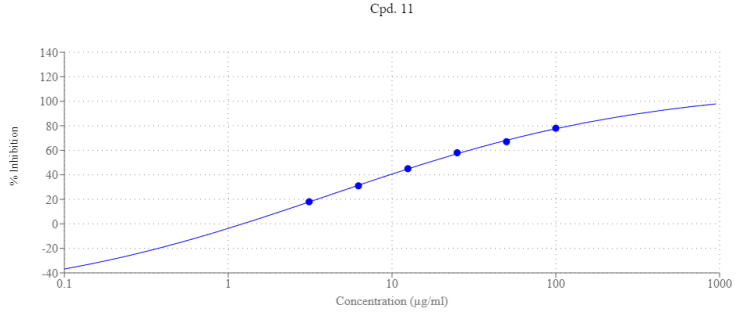 Cpd. 11 % Inhibition Concentration (µg/ml)	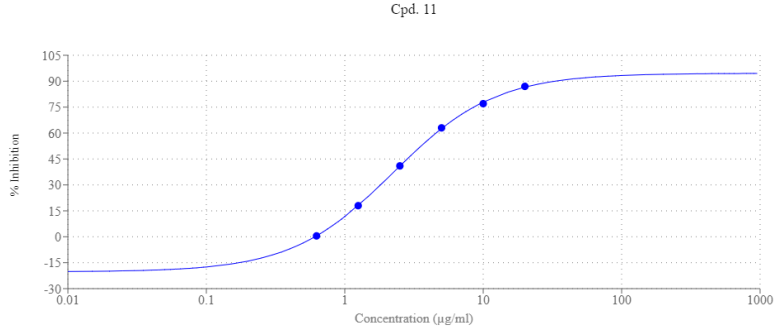 Cpd. 11 % Inhibition Concentration (µg/ml)

12	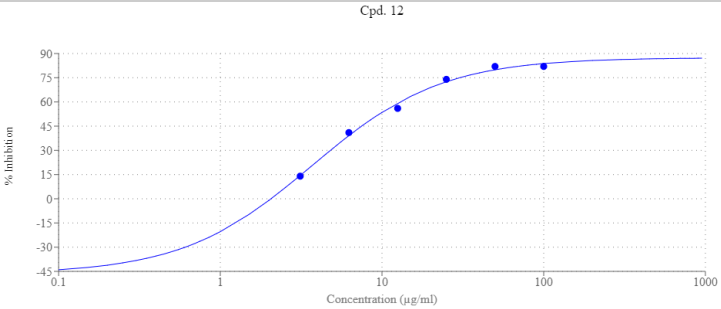 Cpd. 12 % Inhibition Concentration (µg/ml)	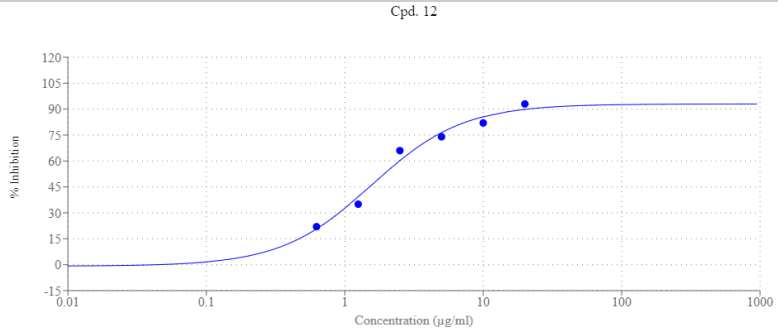 Cpd. 12 % Inhibition Concentration (µg/ml)
13	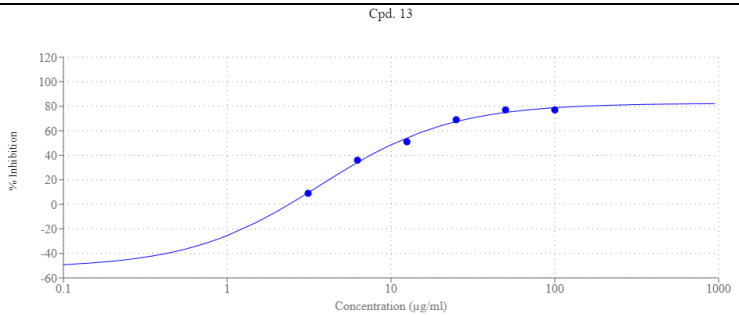 Cpd. 13 % Inhibition Concentration (µg/ml)	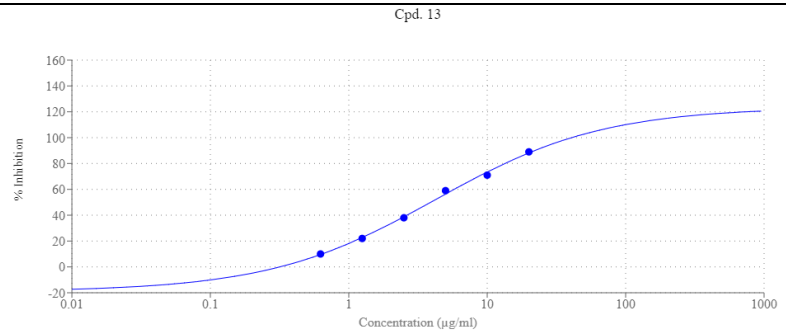 Cpd. 13 % Inhibition Concentration (µg/ml)
14	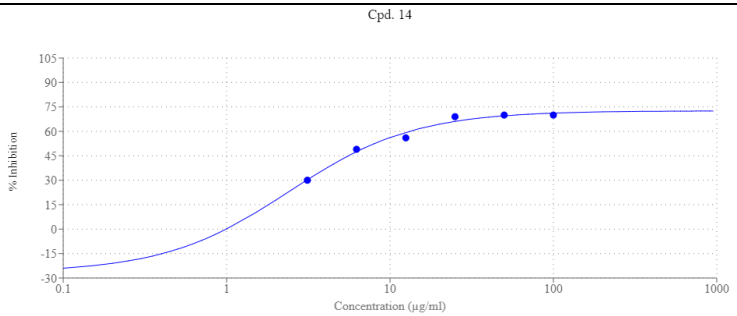 Cpd. 14 % Inhibition Concentration (µg/ml)	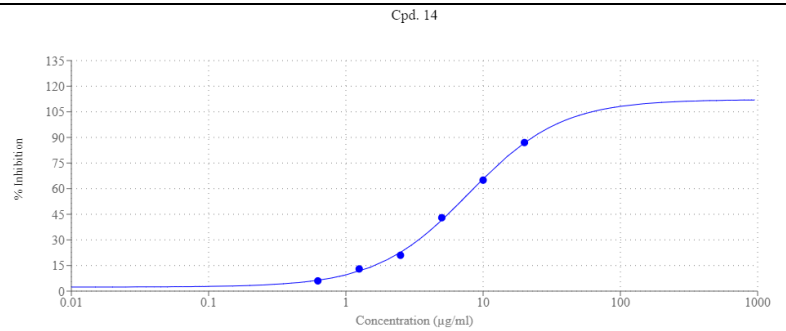 Cpd. 14 % Inhibition Concentration (µg/ml)
15	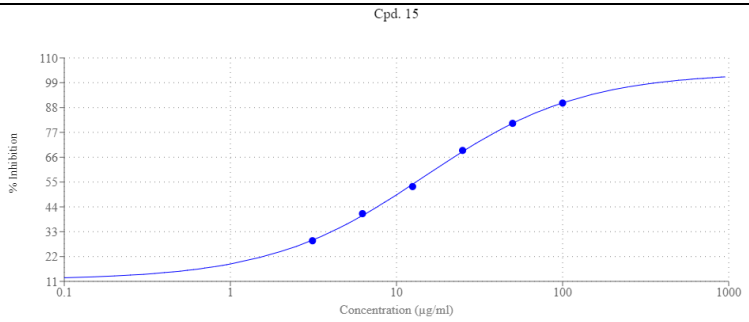 Cpd. 15 % Inhibition Concentration (µg/ml)	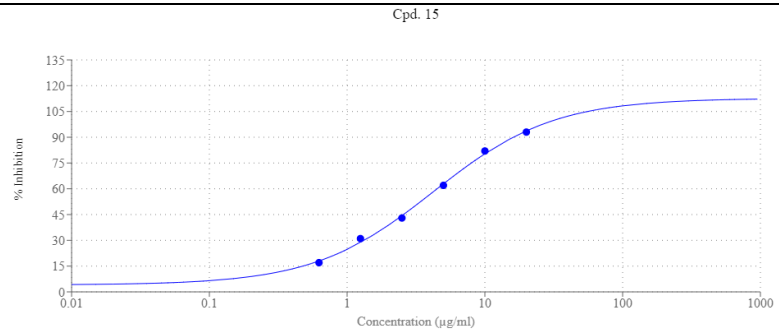 Cpd. 15 % Inhibition Concentration (µg/ml)

16	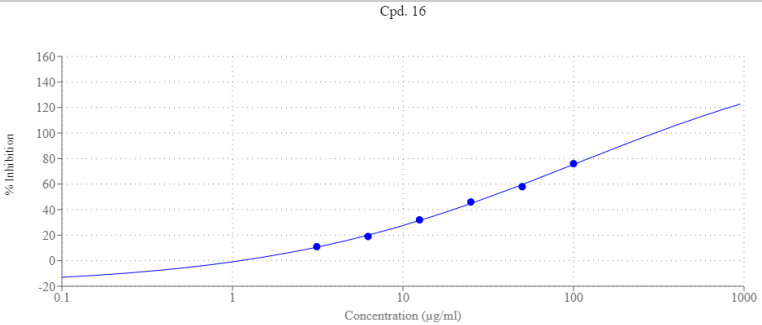	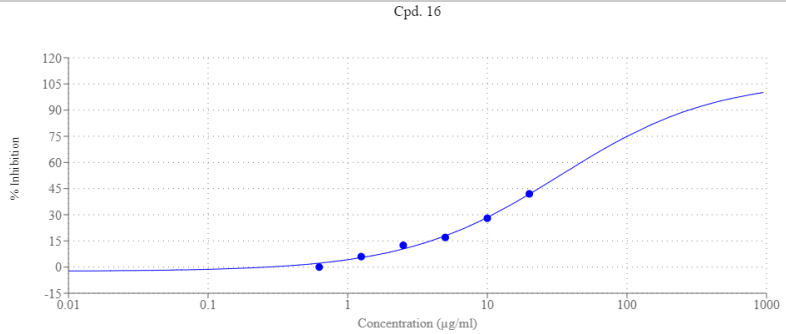
17	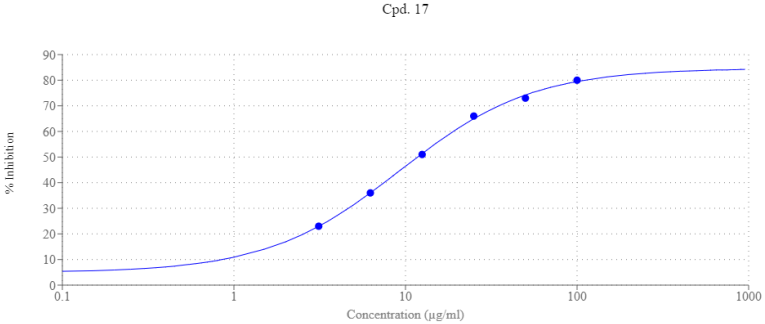	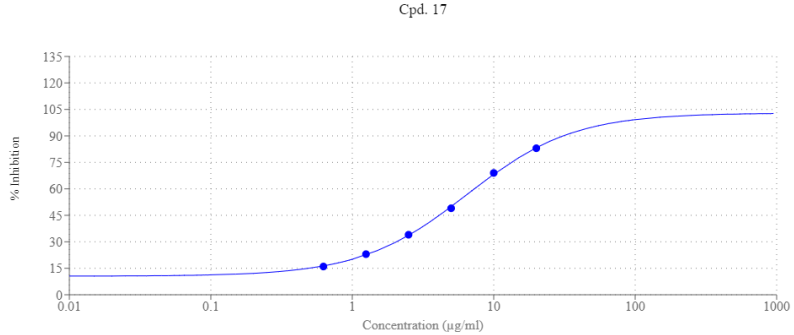
18	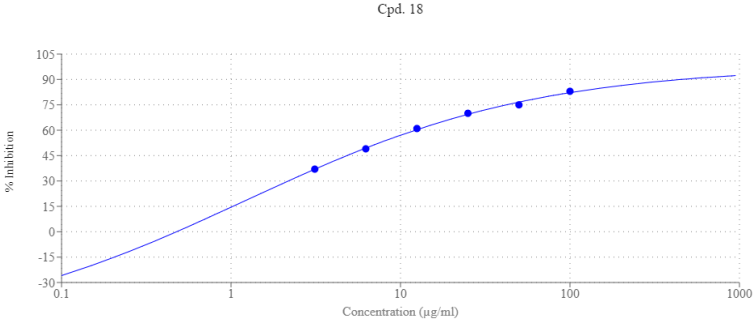	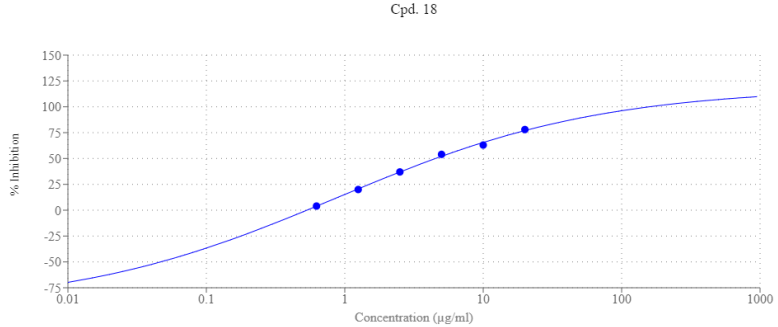
Sorafenib	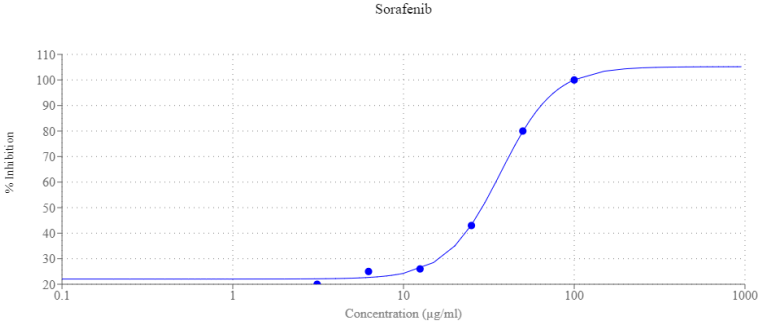	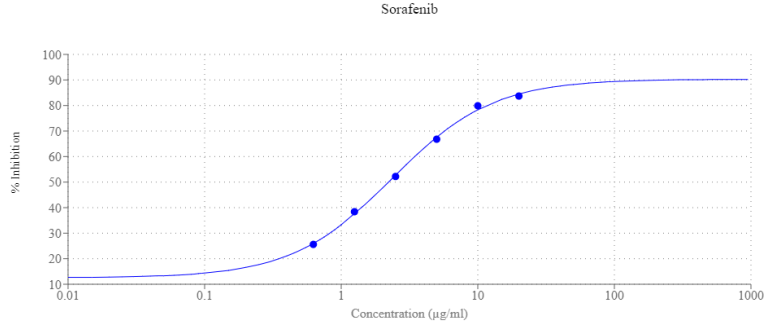

3.2. Mechanistic study:

3.2.1. qRT-PCR analysis for EGFR/PI3K/mTOR/Bcl-2/Bax/P53 genes in A549 cell line

$5*10^4$ cells were seeded into each well of a 12-well plate and then incubated in a CO_2-rich incubator (37°C, 5% CO_2, and 90% relative humidity) for a whole day. After the incubation time, 750 µL of the IC_{50} concentration of each test compound was added to the plate, and it was further incubated for 24 h in the CO_2 incubator (37°C, 5% CO_2, and 90% relative humidity). The plate was centrifuged at 1650 rpm for 5 min., and the supernatants were discarded. Following the incubation period, the cell plate underwent RNA isolation using an RNA isolation kit (iNtRON Biotechnology, Korea) according to the manufacturer's instructions.

RNA was then converted into cDNA using the sensiFAST cDNA synthesis kit (Bioline, London). B-actin served as the housekeeping gene in the qPCR gene amplification process. 12.5 µL of SensiFAST SYBR (Bioline, London) was mixed with 1µL of cDNA, 0.5 µL forward primer (10 pmoles/ml), and 0.5 µL reverse primer (10 pmoles/ml) for each primer (Table 4). The volume was adjusted to 20 µL using nuclease-free distilled water. Samples were then placed in the CFX96TM Real-Time System (BIO-RAD, USA), and the program started with an initial denaturation cycle at 95°C for 10 min, followed by 40 cycles of denaturation at 95°C for 15 sec, annealing at 60°C for 30 sec, and extension at 72°C for 30 sec. The fold change in target genes was determined using the $2^{-\Delta\Delta CT}$ method to normalize the critical threshold (C_t) quantities of the target gene with the C_t quantities of the housekeeping gene.

Table S4: Sequence of primers for mutational analysis of EGFR, PI3K, mTOR, Bcl-2, Bax and p53 genes

PI3K	Forward: 5’-CTG CCTGCG ACAGATGAG TG-3
	Reverse: 5’-TCCGAT TACCAAGTG CTC TTTC-3
mTOR	Forward: 5’-ACA ACT TTG GTATCG TGG AAGG-3’
	Reverse: 5’-GCC ATC ACG CCACAG TTTC-3’
EGFR	forward: 5'-TGGAGC TACGGG GTGACCGT-3
	Reverse: 5'-GGT TCAGAG GCT GAT TGT GAT-3
Bcl-2	Forward: 5’-ATG TGTGTG GAG AGCGTC AACC-3’
	Reverse: 5’-CAG AGACAG CCAGGAGAA ATCAA-3’
Bax	Forward: TCAGGATGCGTCCACCAAGAAG
	Reverse: TGTGTCCACGGCGGCAATCATC
P53	Forward: CCTCAGCATCTTATCCGAGTGG
	Reverse: TGGATGGTGGTACAGTCAGAGC
B-actin	Forward: 5’-TCA AGA AGG TGG TGA AGC AGG-3’
	Reverse: 5’-AGCGTC AAAGGTGGAGGAGTG-3’

3.2.2. Apoptosis investigation

3.2.2.1. Flow cytometric analysis

Overnight, A549 cells were seeded in 6-well culture plates at a density of 3-5× 10^3 cells/well and incubated. Compound **8** was then applied to the cells at its IC_{50} value and left on for 48 hours. After incubation, the cells and supernatants were washed with ice-cold PBS. The cells were then resuspended in 100 µL of annexin binding buffer solution (25 mM $CaCl_2$, 1.4 M NaCl, and 0.1 M Hepes/NaOH, pH 7.4) and incubated with Annexin V-FITC (1:100) and propidium iodide (PI) at a concentration of 10 µg/mL for 30 minutes in the dark. The stained cells were then analyzed using a BD FACSCalibur™ Flow Cytometer.[3-6]

3.2.2.2. Determination of caspases 3, 7, 8 and 9

Briefly, A549 (Lung carcinoma) cells were cultured to a confluent monolayer and then treated with the tested samples at the IC_{50} concentration as described earlier. After 48 h of treatment, the cells were harvested by trypsinization with 0.25% trypsin, followed by centrifugation for 5 min. The cell pellets were then washed twice with PBS for 20 min. each and resuspended in binding buffer. Apoptotic markers in both treated and untreated A549 cells were examined. The levels of caspase-3, caspase-7, caspase-8, and caspase-9 were assessed using ELISA colorimetric kits following the manufacturer's instructions. Specifically, the ELISA kits used were as follows: Human caspase-3 (Cat. No.: E-EL-H0017) from Elabscience, Human caspase-8 (Cat. No.: E-EL-H0659) from Elabscience, Human caspase-9 (Cat. No.: E-EL-H0663) from Elabscience, and Human Caspase 7 (Cat. No.: NBP2-75037) from Novus Biologicals USA.

Table S5: Determination of Caspases (ng/ml) by ELISA in A549 cell line as fold change for the most active compound 8

ID	Caspase 3 (ng/ml) At three independent readings			Mean Caspase3 levels (ng/ml) ± S.D.	Caspase 7 (ng/ml) At three independent readings			Mean Caspase 7 levels (ng/ml) ± S.D.	Caspase 8 (ng/ml) At three independent readings			Mean Caspase 8 levels (ng/ml) ± S.D.	Caspase 9 (ng/ml) At three independent readings			Mean Caspase 9 levels (ng/ml) ± S.D.
	1st	1st	1st		1st	1st	1st		1st	1st	1st		1st	1st	1st	
Cpd.8	6.78	6.96	7.01	6.92±0.12	89.06	90.73	92.14	90.64±1.54	123.56	120.94	118.75	121.08±2.41	45.32	44.96	43.87	44.72±0.76
Control	3.81	4.23	3.98	4.01±0.21	68.41	68.06	66.83	67.77±0.83	56.27	54.86	53.91	55.01±1.19	43.17	43.88	42.95	43.33±0.49

3.2.3. Investigation of PI3K and mTOR enzymatic activity

PI3K-α (cat.#40639),[7] and mTOR (cat.#CBA055)[8] kinase inhibition assays were conducted using ELISA kits according to the manufacturer's instructions. To assess the inhibitory potency of compound **8** against kinase activity, kinase inhibitory tests were carried out. The percentage inhibition of autophosphorylation was calculated using the following formula: $100-[(A_{Control})/(A_{Treated}) - A_{Control}]$.[3, 9] The IC_{50} values were then determined by plotting inhibition percentages at five different concentrations using the GraphPad Prism 7 software.

3.2.3.1. Dose-response curve for PI3K and mTOR enzymatic activity

PI3K
ΔT=30 min **compound 8= 618.68**

Compound [μM]	Cont.	10	5	2.5	1	0.1	0.01
8	0.751	0.03	0.21	0.29	0.349	0.423	0.645
	0.742	0.02	0.2	0.28	0.349	0.417	0.643
	0.728	0.01	0.22	0.29	0.376	0.419	0.658
Mean	0.740333	0.02	0.21	0.286667	0.358	0.419667	0.648667
SD	0.011059	0.01	0.01	0.005774	0.015588	0.003055	0.008145
% of valibility	100	2.701486	28.3656	38.72 13	48.35 66	56.68618	87.61819
% of inhibition	0	97.29851	71.6344	61.27 87	51.64 34	43.31382	12.38181

mTOR
ΔT=30 min **compound 8= 618.68**

Compound [μM]	Cont.	10	5	2.5	1	0.1	0.01
8	0.768	0.019	0.128	0.278	0.299	0.311	0.659
	0.765	0.018	0.146	0.276	0.289	0.328	0.653
	0.769	0.017	0.176	0.276	0.298	0.327	0.653
Mean	0.767333	0.018	0.15	0.276667	0.295333	0.322	0.655
SD	0.002082	0.001	0.024249	0.001155	0.005508	0.009539	0.003464
% of valibility	100	2.345786	19.54822	36.0556	38.48827	41.96351	85.36056
% of inhibition	0	97.65421	80.45178	63.9444	61.51173	58.03649	14.63944

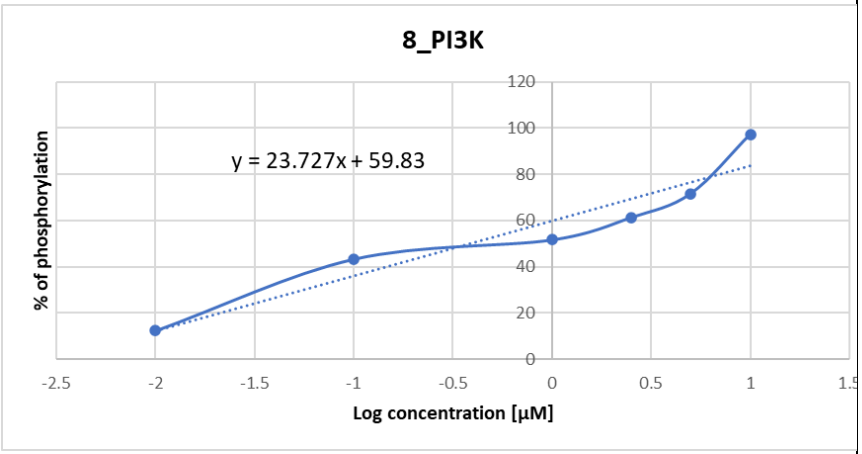

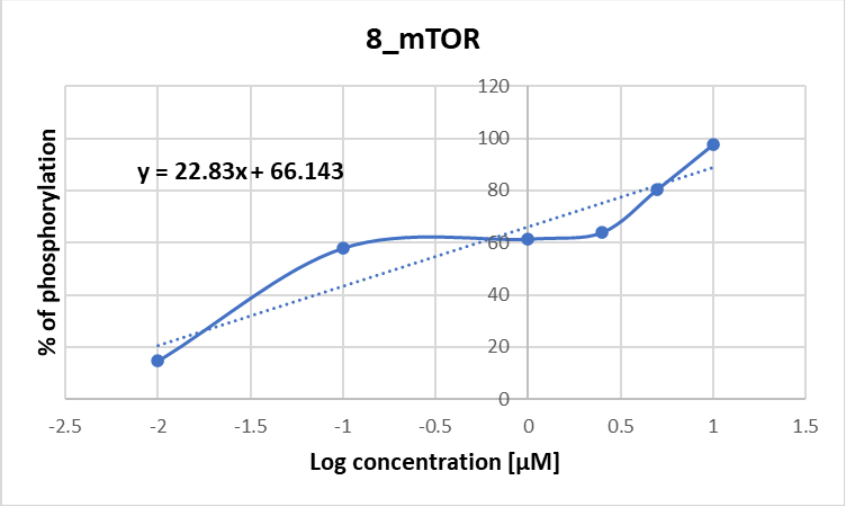

Fig. S19: Dose-response curve of log concentration [uM] versus perecntage of phpsphorylation following PI3K(#40639) and mTOR (No. CBA05). The dotted line is linear regression curve fit using EXCEL.

4. Molecular docking study

Vina Autodock[11] was employed to conduct a docking investigation. The crystal structures of the specific domains of PI3K-α (PDB: 4JPS),[12], and mTOR (PDB: 4JT5)[13] were retrieved from the Protein Data Bank (PDB). During the docking procedure, the studied compounds and target proteins were converted to a pdbqt format. The grid box that encircles the binding site was subsequently measured and assessed using the M.G.L. techniques. The docking results were then analyzed and visualized using the Biovia discovery-studio 2021 visualizer[14] to generate 3D and 2D anticipated binding poses for the evaluated compounds.

5*. Data analysis and statistics*

The data are expressed as mean ± standard error of mean (SEM) and the significant values were considered at $p < 0.05$. One-way analysis of variance (ANOVA) by Tukey's test used for evaluating the difference between the mean values of the studied treatments.[15] The analysis was done for three measurements using SPSS software version 16.

6. References

[1] T. Mosmann, Rapid colorimetric assay for cellular growth and survival: application to proliferation and cytotoxicity assays, Journal of immunological methods 65(1-2) (1983) 55-63.
[2] A.B. Inc., IC_{50} Calculator, 2024. https://www.aatbio.com/tools/ic50-calculator.
[3] I. Shawish, A. Barakat, A. Aldalbahi, A.M. Malebari, M.S. Nafie, A.A. Bekhit, A. Albohy, A. Khan, Z. Ul-Haq, M. Haukka, Synthesis and antiproliferative activity of a new series of mono-and bis (dimethylpyrazolyl)-s-triazine derivatives targeting EGFR/PI3K/AKT/mTOR signaling cascades, ACS omega 7(28) (2022) 24858-24870.
[4] M.S. Nafie, S.M. Kishk, S. Mahgoub, A.M. Amer, Quinoline-based thiazolidinone derivatives as potent cytotoxic and apoptosis-inducing agents through EGFR inhibition, Chemical Biology & Drug Design 99(4) (2022) 547-560.
[5] M.S. Goda, M.S. Nafie, B.M. Awad, M.S. Abdel-Kader, A.K. Ibrahim, J.M. Badr, E.E. Eltamany, In vitro and in vivo studies of anti-lung cancer activity of Artemesia judaica L. crude extract combined with LC-MS/MS metabolic profiling, docking simulation and HPLC-DAD quantification, Antioxidants 11(1) (2021) 17.
[6] M.S. Nafie, N.H. Elghazawy, S.M. Owf, K. Arafa, M.A. Abdel-Rahman, R.K. Arafa, Control of ER-positive breast cancer by ERα expression inhibition, apoptosis induction, cell cycle arrest using semisynthetic isoeugenol derivatives, Chemico-Biological Interactions 351 (2022) 109753.
[7] https://bpsbioscience.com/pi3-kinase-p110-k111n-p85-recombinant-40639; (Accessed September 2024).

[8] https://www.merckmillipore.com/INTL/en/product/K-LISA-mTOR-Activity-Kit,EMD_BIO-CBA055; (Accessed September 2024).

[9] E.E. Salama, M.F. Youssef, A. Aboelmagd, A.T. Boraei, M.S. Nafie, M. Haukka, A. Barakat, A.A. Sarhan, Discovery of Potent Indolyl-Hydrazones as Kinase Inhibitors for Breast Cancer: Synthesis, X-ray Single-Crystal Analysis, and In Vitro and In Vivo Anti-Cancer Activity Evaluation, Pharmaceuticals 16(12) (2023) 1724.
[10] A. Grada, M. Otero-Vinas, F. Prieto-Castrillo, Z. Obagi, V. Falanga, Research techniques made simple: analysis of collective cell migration using the wound healing assay, Journal of Investigative Dermatology 137(2) (2017) e11-e16.
[11] O. Trott, A.J. Olson, AutoDock Vina: improving the speed and accuracy of docking with a new scoring function, efficient optimization, and multithreading, Journal of computational chemistry 31(2) (2010) 455-461.
[12] P. Furet, V. Guagnano, R.A. Fairhurst, P. Imbach-Weese, I. Bruce, M. Knapp, C. Fritsch, F. Blasco, J. Blanz, R. Aichholz, Discovery of NVP-BYL719 a potent and selective phosphatidylinositol-3 kinase alpha inhibitor selected for clinical evaluation, Bioorganic & medicinal chemistry letters 23(13) (2013) 3741-3748.
[13] H. Yang, D.G. Rudge, J.D. Koos, B. Vaidialingam, H.J. Yang, N.P. Pavletich, mTOR kinase structure, mechanism and regulation, Nature 497(7448) (2013) 217-223.
[14] B. Dassault, Systemes, Discovery studio visualizer, version v21. 1.0. 20298, Dassault Systemes, San Diego (2021).
[15] Kotz S, Balakrishnan N, Read CB, V. B, Encyclopedia of statistical sciences. 2nd ed. Hoboken, N.J.: Wiley-Interscience, 2006.